Development of a Self-Optimization Framework of Reactive Units for Energy Efficient Operation of a Petroleum Refinery

By

Abdul Samad

School of Chemical and Materials Engineering

National University of Sciences and Technology

2022

Development of a Self-Optimization Framework of Reactive Units for Energy Efficient Operation of a Petroleum Refinery

Name: Abdul Samad

Reg No: 00000328097

This work is submitted as an M.S. thesis in partial fulfillment of the requirement for the degree of

M.S. in Process Systems Engineering

Supervisor Name: Dr. Iftikhar Ahmad

School of Chemical and Materials Engineering (SCME)

National University of Sciences and Technology (NUST)

H-12 Islamabad, Pakistan

December 2022

I have devoted my thesis to my family constant support, encouragement, love, and honour.

Acknowledgment

All praise and eminence are due to "ALLAH," the undisputed architect of this world, who gave us the capacity for comprehension and sparked our curiosity about the planet as a whole. Warmest welcomes to the supreme ruler of this world and the hereafter, "Prophet Mohammed (PBUH)," a source of knowledge and benefits for all of humanity as well as for Uma.

I would like to acknowledge and express my sincere gratitude to my research **supervisor**, **Dr. Iftikhar Ahmad** for his endless support, supervision and affectionate guidance to steer me in the right the direction whenever he thought I needed it. I would also like to extend my gratitude to **committee members**; **Dr. Muhammad Nouman Aslam** and **Dr. Nouman Ahmad**. for their valuable suggestions and guidance.

I would also like to thank **Prof. Dr. Amir Azam Khan** (Principal School of Chemical and Materials Engineering) and **Dr. Erum Pervaiz** (HOD Department of Chemical Engineering) for providing a research oriented platform to effectively utilize my skills in accomplishing this research work.

In the end, I must express my very profound gratitude to my parents for providing me with unfailing support and continuous encouragement throughout my years of study and through the process of researching and writing this thesis. This accomplishment would not have been possible without them.

Abdul Samad

Abstract

In this work, integrated frameworks of the artificial neural networks (ANN) with genetic algorithm (GA) and particle swarm optimization (PSO) were developed to realize higher exergy efficiency of reactive units of a refinery under uncertainty in process conditions. Initially, a steady-state Aspen model was used to perform exergy analysis for quantifying exergy efficiency, irreversibility and improvement potential of the plant. The process model was then transformed to a dynamic mode by inserting ±5% uncertainty in process conditions, i.e., temperature, pressure, and mass flow rate, to generate a dataset of 216 samples for integrated naphtha and isomerization process and 200 for delayed coking process. An ANN model was developed using the dataset to predict exergy efficiency. The ANN model was used as a surrogate in GA and PSO environments to achieve higher exergy efficiency under uncertainty. The optimized process condition derived through GA and PSO based approach were fed to Aspen model for cross-validation. The integrated naphtha and isomerization process had an overall exergy efficiency, irreversibility, and improvement potential of 50.57%, 34955.55 kW, and 17276.98 kW, respectively. Whereas the delayed cocking process had an overall exergy efficiency, irreversibility, and improvement potential of 77.61%, 29204.035 kW, and 6539.51 kW, respectively. The correlation coefficient of ANN model was 0.97432 for integrated naphtha and isomerization process and 0.99051 for delayed coking process. Performance of the GA and the PSO based approaches were comparable, and they significantly enhanced the exergy efficiency of the plant when compared to standalone Aspen model of the process.

Keywords: Artificial Neural Network, Genetic Algorithm, Exergy efficiency, Exergy destruction, Irreversibility, Delayer cocker, Naphtha reforming. isomerization; Uncertainty, Energy recovery; Machine learning

``

Table of Contents

List of Figures

List of Tables

Nomenclature

Y_i	Predicted value
η	Exergy efficiency
AI	Artificial intelligence
ANN	Artificial Neural Networks
B	Bias
BF	Bootstrap filter
CFD	Computational fluid dynamics
DIH	De-iso-hexanize
DIP	De-iso-pentanizer
DP	De-pentanize
DT	Decision trees
Ex_{che}	Chemical exergy
$Ex_{destroyed}$	Exergy destruction
Ex_{feed}	Feed exergy
Ex_{heat}	Heat exergy
Ex_{in}	Exergy in
Ex_{out}	Exergy out
Ex_{ph}	Physical exergy
$Ex_{product}$	Product exergy
Ex_s	Total exergy of stream
Ex_{work}	Work exergy
f	Activation function
GA	Genetic Algorithm
H	Enthalpy
H_0	Standard Enthalpy
I	Irreversibility
IP	Improvement potential
RMSE	Root means squared error
P	Pressure
P0	Standard pressure

Qc	Condenser duty
Qr	Reboiler duty
R^2	Coefficient of determination
RF	Random forests
RON	Research octane number
S	Entropy
S_0	Standard Entropy
T	Temperature
T_0	Standard temperature
Tc	Condenser temperature
Tr	Reboiler temperature
VDU	Vacuum distillation unit
wi	Weights
xi	Inputs

Chapter 1

Introduction

1.1 Background

Globally the depletion of fossil reservoirs, environmental concerns, rapid growth in industrialization, and the associated rise in energy demand and utilization have solicited the feasible usage of energy [1, 2]. Energy is the lifeline of the modern world, and the petrochemical sector is its backbone. Consumer chemicals, specialized chemicals, and basic chemicals are the three primary products of the petrochemical industry covers a vast array of goods in sectors ranging from energy, buildings, transportation, pharmaceutical, electronics and telecommunication. As the largest sector and the energy-intensive nature of its production processes, it accounted for around 37% of the world's energy consumption and about 13% of the world's greenhouse gas emissions (GHG). Furthermore, a 40% rise in consumption is anticipated till 2040, as shown in Figure 1.

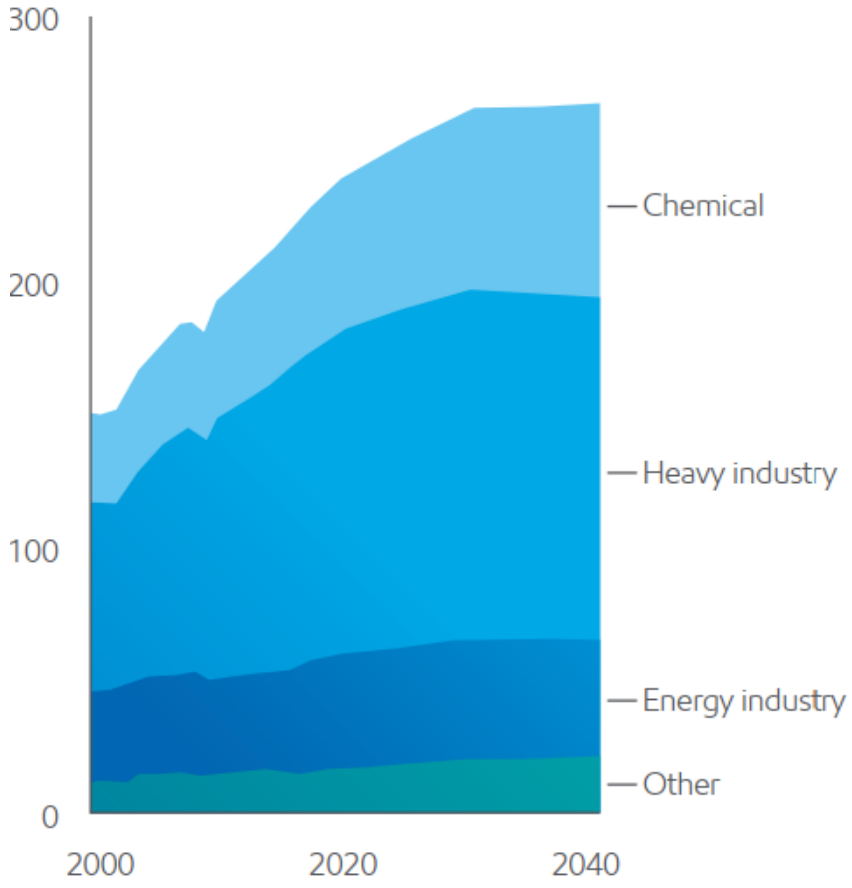

Figure 1: Forecast of industrial energy demand by 2040 [3]

Among various petrochemical industries, petroleum refinery is one of the most energy-intensive consuming 33% of total industrial energy. According to the US Department of Energy, a 794 TBTU/year (26%) of energy can be recovered if current RD-based technologies are deployed efficiently in US oil refineries [4, 5]. Figure 2 displays potential energy-saving opportunities in the petroleum refinery. As depicted from Figure 2, the major opportunities for saving energy are in reactive units i.e. catalytic reforming, coking, isomerization, hydrocracking and hydrotreating. So, improving the energy efficiency of the processes is always desired to make them more viable and sustainable.

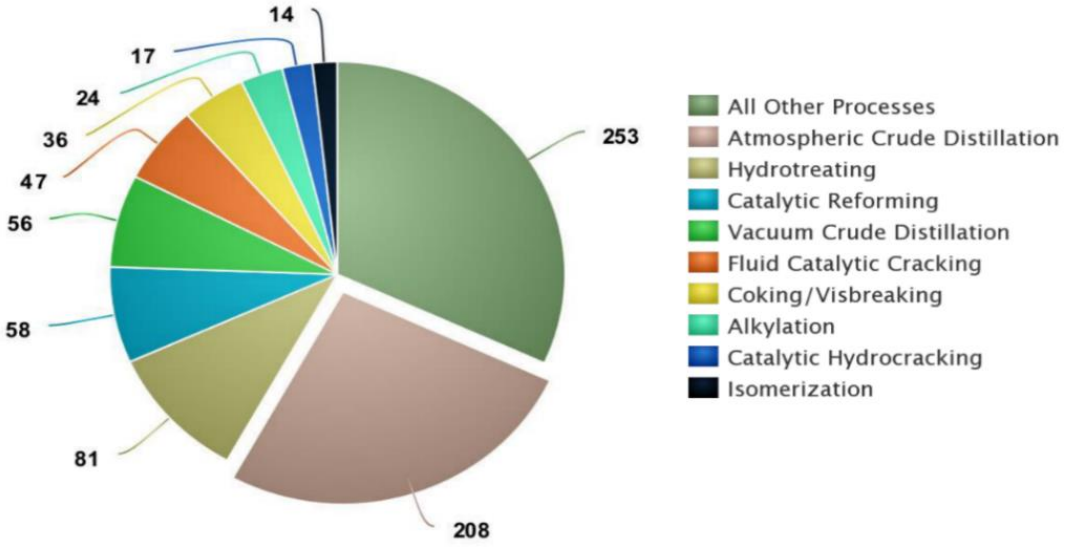

Figure 2: Potential of Energy saving in U.S. petroleum refinery [4, 5]

The analysis of identifying energy losses and improvement potential can be broadly divided into two categories. One is based on conventional energy analysis, which relies solely on the first law of thermodynamics and simply measures the amount of energy wasted relative to the amount of energy put in without considering the energy's quality or its potential for driving a process. [6]. While the other is based on exergy analysis, which integrates the first and second laws of thermodynamics to identify the true thermodynamic improvement potential within the process [7, 8].

Exergy analysis is a potential tool that can accurately identify the location, magnitude, and cause of energy degradation in the process. Furthermore, it allows engineers to find the individual performance of each component, providing room for improvement and potential for cost savings. Process enhancement through exergy analysis results in the feasible use of natural resources and hence green processes. The use of exergy

analysis is broadly studied to assess, design, and optimize the performance of various industrial processes like chemical [9], sugar [10], cement [11], steel [12], pulp, and paper [13], and petrochemical [14]. However, the method of exergy calculation faces challenges in coping with uncertainty in process conditions because of the complexities of modeling tasks and high computational time. This research aims to develop a computational model that can efficiently be utilized during the chemical industries' designing or operational stage to deal with uncertainty. This tool should be rigorous enough to handle the complicated calculations required for exergy analysis while still being adaptable enough to be modified as needed.

1.2 Objectives

The objectives of the thesis are given below,

- Exergy analysis of reactive units to quantify the process's irreversibilities, exergy efficiencies, and improvement potentials.
- Development of ANN model for data-based prediction of exergy efficiency of the process under uncertainty.
- Use of the ANN model as a surrogate in GA and PSO frameworks to realize higher exergy efficiency of the process under uncertainty.

1.3 Thesis Outline

The thesis is organized as follows. Chapter 1 describes the background, followed by chapter 2, which gives a detailed literature review. Chapter 3 discusses the research methodology to develop the framework to predict and optimize the exergy efficiency. Chapter 4 contains the results and discussions about exergy quantification and the optimization framework.

Chapter 2

Literature Review

2.1 Literature Review

The integrated naphtha reforming and isomerization, and delayed cocker are the three essential processes in petroleum refineries because of the high demand for their products. Naphtha reforming converts crude naphtha with low-octane fuels such as paraffin and naphthene into high-octane fuel and aromatic-rich compounds. Isomerization enhances gasoline research octane number (RON) by converting straight-chain paraffin into a branch chain and simultaneously decreasing the benzene content through benzene saturation [15, 16]. Delayed cocking, thermally crack heavy residue into desired products [17].

The integrated naphtha reforming, isomerization, and delayed coking processes are energy intensive. So, improving the energy efficiency of the processes is always desired to make them more viable and sustainable. The analysis of identifying energy losses and improvement potential can be broadly divided into two categories. One is based on the conventional approach of energy analysis using the first law of thermodynamics, while the second is based on exergy analysis that integrates the first and second laws of thermodynamics to identify the true thermodynamic improvement potential within the process.

Various studies based on the first law of thermodynamics have been reported on naphtha reforming, isomerization, and delayed coking processes. For instance, Liang et al. [18] based on pinch and retrofit analysis, suggested an alternate heat exchanger network design to save up to 7595 kW energy. The saved energy account for 14.6% of hot utility consumption and 22.3% of cold utility consumption. Ulyev et al. [19] minimize the energy consumption of 6.4 MW by implementing the proposed retrofit through pinch analysis. The analysis reduced 35.5% hot utility consumption and 51.9% cold utility consumption.

Babaqi et al. [20] applied pinch analysis with particle swarm optimization and almost reduced 16.20% of utility demand by adding additional area to the heat exchanger, which led to fast energy recovery. Falcon et al. [21] applied the Six Sigma Define, Measure, Analyse, Improve and Control (DMAIC) methodology to improve the

energy efficiency of the distillation units, savings more than 157,000€/year. They defined energy efficiency indicator in the define phase, and structure the data in useful information in the measurement phase, establishing the baseline against which all future improvements will be compared. In the analysis phase they identified 14 critical inputs to correct variation in a process. In the end, they validates the optimization results with baseline in the improvement phase.

Velázquez et al. [22] developed and implemented an energy management system based on data mining. The data mining approach found major influential variables and modeled this variabled to characterize plant energy performance. From 45 influential variables, 14 major influential variables were selected and were modeled for energy performance indicators, increasing energy efficiency from 27% to 32%.

Pinch analysis has also been used to reduce the energy consumption of the isomerization process. For instance, Feng et al. [23] proposed a heat exchanger network based on pinch analysis with energy-saving potential accounting for 34.2% of current heat utility consumption. Ghazizahed et al. [24] studied two scenarios of energy pockets and heat pump based on pinch and retrofit analysis to enhance heat transfer in the isomerization process to save energy and cost. Results depict that the energy pocket reduces medium pressure (MP) steam consumption and increased energy recovery due to a large driving force. Whereas the heat pump minimized both cooling water and low-pressure steam consumption.

Jarullah et al. [25] achieved heat saving of 25.2% with heat integration through pinch analysis in the heat exchanger network of the AJAM isomerization process. The saved energy account for 11.465% of hot utility consumption and 8.9% of cold utility consumption. Ghazizahed el al. [26] applied pinch analysis to three different scenarios of integrating de-pentanizer (DP), de-iso-pentanizer (DIP), and de-iso-hexanizer (DIH), and concluded that with the increase in quality and quantity of gasoline, the energy consumption of the process increases.

Pinch analysis has also been used to reduce the energy consumption of the delayed coking process. Li et al. [27] based on pinch and retrofit analysis, suggested an alternate heat exchanger network with an energy-saving potential accounting for 19 % of the hot utility demand and 6378 tons/year of fuel consumption. Lie et al. [28] developed a mixed integer linear programming model (MILP) to simultaneously

optimize the complex fractional column and heat exchanger network and reduced the the total annual cost by 2.1 million CYN. Sidenev et al. [29] based on pinch and retrofit analysis, suggested an alternate heat exchanger network design to save up to 1576 kW energy.

Energy analysis based on second law of thermodynamics also termed as exergy analysis is getting the attention of researchers due to its capability to quantify process irreversibility and true improvement potential. Several studies have been reported on naphtha reforming and delayed coking process. For instance, Rivero et al. [30], through exergy analysis, quantified that the naphtha reforming unit contributes 10.9% to the total exergy destruction of the refinery. Parath et al. [31] applied exergy analysis with life cycle assessment on naptha reforming and found heat exhangers were the main source of exergy destruction.

Another study was conducted by Mustafa et al. [32] in the reactors of a naphtha reforming unit. The exergy analysis along the reactor length was analyzed, and it was found that the chemical exergy increased, and the physical and mixing exergy decreased with an increase in reactor length because of products high chemical potential. Chen et al. [33] introduced a three-link structural model to reduce energy and exergy losses. The model reduced 37.2% of energy consumption by energy-saving measures anticipated as per the energy use of the structural model. Lei et al. [34] applied a novel diagram representation approach based on an advanced energy level composite curve with the concept of avoidable and unavoidable exergy destruction. Results showed fractional column had the highest improvement potential of 38.1%.

In the current trend of artificial intelligence (AI) applications in process industries, the use of a data-based approach has also been reported for exergy analysis on various process units. Arif et al. [35] developed an machine-learning model to predict the blast furnace's exergy efficiency. First, they performed a steady state exergy analysis and found the furnace at high temperature was the most exergetic. Then they developed ANN model from data generated under artificial uncertainty in the elven process condition of the first principal model.

In another study, Khan et al. [36] developed straight run (SR) GA and ANN models to study the effect of artificial uncertainty in process conditions and crude composition on exergy efficiency and losses of the furnace while keeping the mass flow rate of oil,

fuel, and excess air constant. Kurban et al. [37] developed machine learning models to predict vacuum distillation unit (VDU) exergy efficiency under elven uncertain process parameters. First, they performed a sensitivity analysis to study the effect of different process parameters on exergy efficiency. They found the exit furnace temperature to be the most influential. Then they developed and compared random forest (RF) and bootstrap aggregating (bagging) models to study the effect of process conditions on exergy efficiency. Akram et al. [38] developed a statistical model based on RF and bootstrap filter (BF) to study the effect of uncertain process conditions on the overall plant exergy efficiency of naphtha reforming. Furthermore, they developed an optimization algorithm by integrating genetic algorithm and ANN.

Although numerous research studies have been published on the steady state exergy analysis of naphtha reforming and delayed coking process, but no work has been reported on the steady state exergy analysis of integrated naphtha reforming and isomerization process to the best of the author's knowledge. Furthermore, no work has been done to optimize the exergy efficiency of both integrated naphtha reforming and isomerization process and delayed coking process under uncertainty.

Chapter 3

Process Description and Methodology

3.1 Process Description

3.1.1 Integrated Naphtha reforming and Isomerization Process

Figure 3 shows a schematic representation of an integrated naphtha reforming and isomerization process. Figure 4 show sub flowsheet of isomerization process. The naphtha reforming model includes 50 kinetic lumping and 115 reactions, and the isomerization model includes 20 lumping and 20 reactions.

Naphtha Reforming. Feeds are mixed in the mixer before entering the splitter, where light end gases below C_4 are separated. After splitter, the feed enters the distillation column where light naphtha is separated from heavy naphtha and sent to the isomerization unit, while the heavy naphtha enters the reaction section. Before entering a cascade of a reactor, both heavy naphtha and hydrogen feed preheated to a reaction temperature. The reaction is endothermic, resulting in a large drop in temperature. So, to maintain the reaction temperature, effluents are heated using the interstage heaters. The effluent from the third reactor is cooled and enters the product separation column, where hydrogen is separated from our desired unstable reformate. Some hydrogen is recycled while the rest is taken as product hydrogen. The unstable reformate is heated and enters the stabilizer, where light gases are separated. Then stable reformate is mixed with the isomerate from the isomerization unit and ends up desired product, gasoline.

Isomerization. Fresh feed (light naphtha) from naphtha reforming is mixed with compressed hydrogen before heating to a reactor inlet temperature. After heating, the feed enters into two fixed bed isomerization reactors where an isomerization reaction occurs. The reaction is reversible and exothermic and occurs at low temperatures due to equilibrium limitation. From the reactor product, off-gas is separated, and un-stabilized isomerate is sent to the stabilizer. In stabilization, light hydrocarbons are separated from the top, and the bottom is taken as our final product.

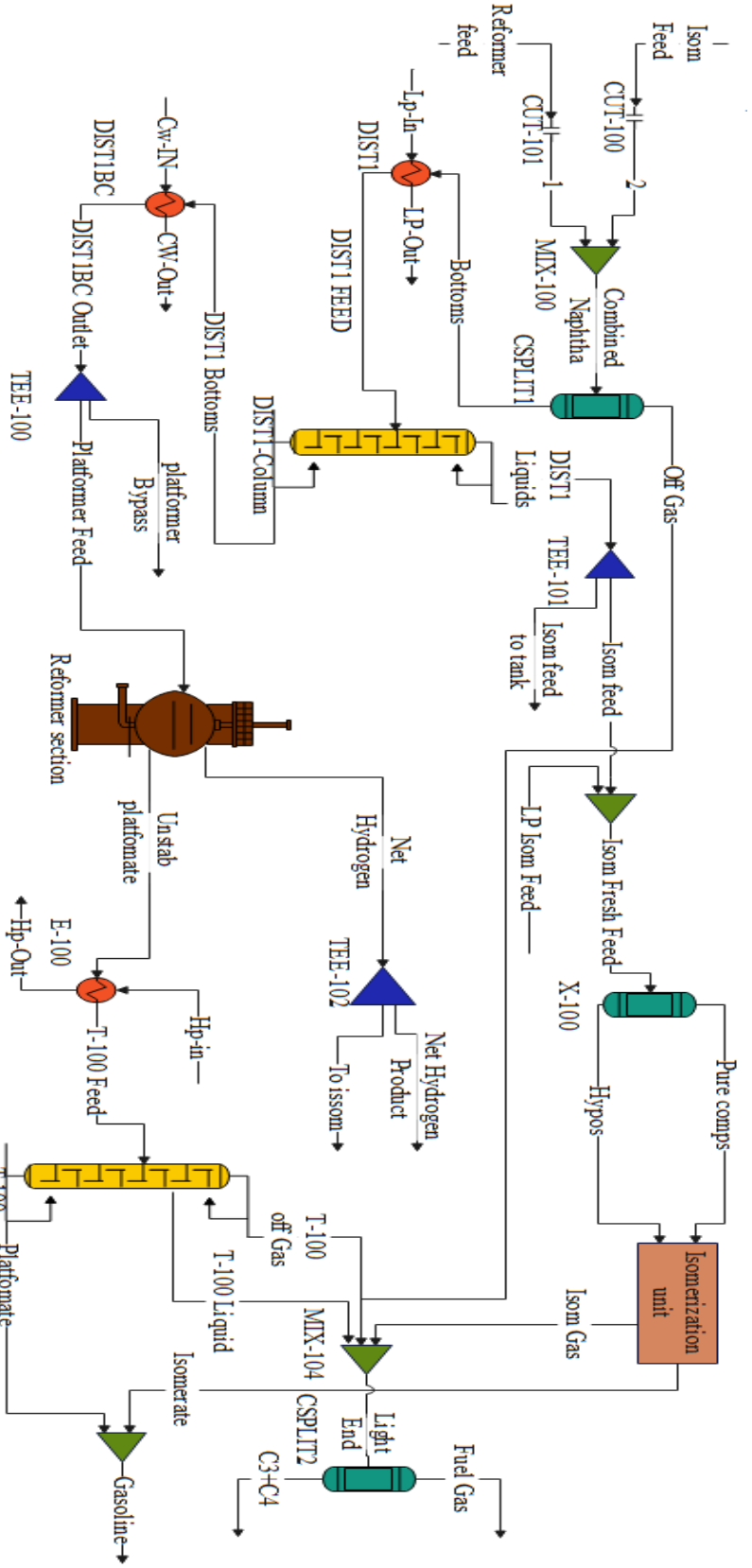

Figure 3: Process flow diagram of integrated naphtha reforming and isomerization process

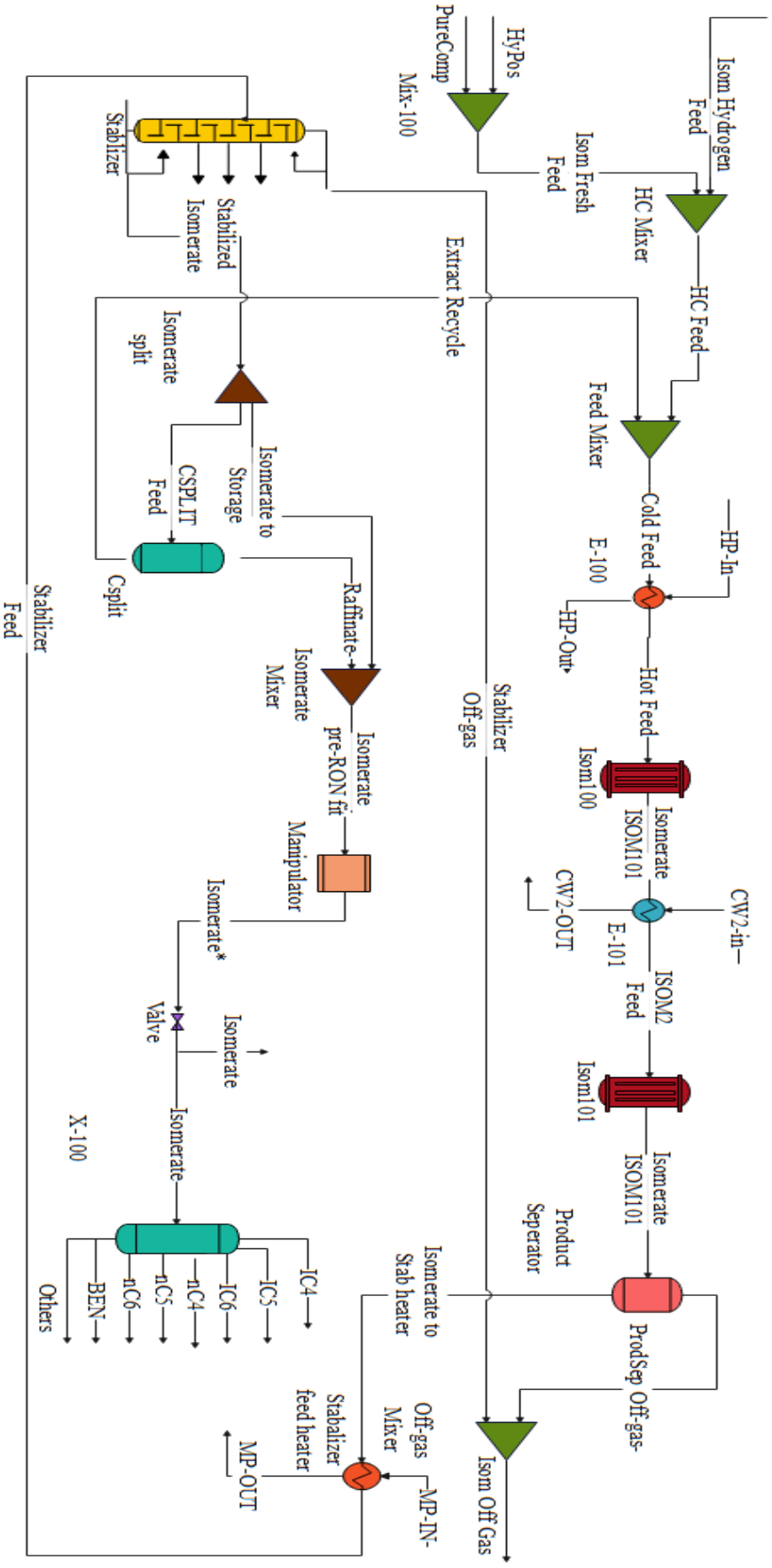

Figure 4: Sub flowsheet of isomerization process

3.1.2 Delayed Coking

A thermal conversion process upgrades the heavy residue into the desired product. The process consists of two coke drums, a furnace, and a fractionator as shown in Figure 5. Vacuum residue as a feedstock enters the bottom of the fractionating column, separating oil lighter than heavy oil and feeding the remaining oil to the coking furnace, which heated it to a temperature of 500^{o}C. Steam is supplied to increase the flow speed to prevent a coking reaction in a furnace. After partial vaporization, the feed enters the coke drum, where our reaction occurs; the drum is insulated for 16-18 hr. The reactors operate alternatively with 24 hours execution cycle in batch mode. When one reactor operates, the other is decoked or cleaned. The coke is removed by injecting steam into the coker drum to remove hydrocarbon vapors, cool it by filling it with water, and then draining it. The hot vapors from the coking drum entered the fractionating column 2-3 plates above the bottom. They are separated based on their boiling points, such as naphtha, wet gas oil, light gas oil, and heavy gas oil. This process handles a variety of feedstock and produces metal and carbon-free products by partial conversion to liquid products. But it has a large amount of coke, 20-30%, with low yield and highly aromatic product, making it expensive.

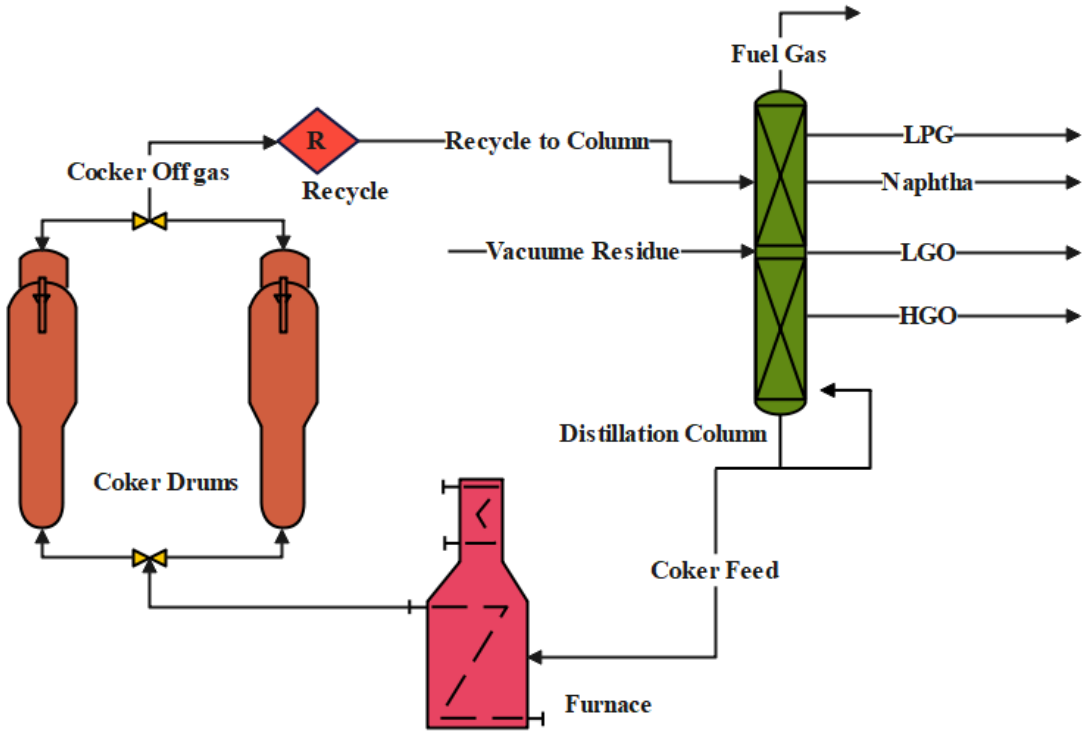

Figure 5: Process flow diagram of delayed cocking process

3.2 Exergy Analysis Formulations

Exergy based analysis incorporates the first and second thermodynamic laws to determine a system's energy-saving potential. It is defined as the maximum useful work a reversible system produces when it is in thermodynamic equilibrium with its surrounding environment [39, 40]. Generally, exergy of a system is comprised of physical exergy and chemical exergy as described in equation (1).

$$Ex_{sys} = Ex_{ph} + Ex_{che} \quad (1)$$

Physical exergy (Ex_{ph}) is the maximum useful work a system produces when it is brought from its initial condition to the environment condition (T_0, P_0) as shown in equation (2).

$$Ex_{ph} = m[(H - H_0 - T_0(S - S)] \quad (2)$$

m, H, and S denote mass flowrate, enthalpy, and entropy at operating conditions and H_0 and S_0 represent enthalpy and entropy at standard conditions

Chemical exergy (Ex_{che}) is the maximum useful work a system produces when it is brought from its environment condition to dead condition as shown in equation (3).

$$Ex_{che} = m[\sum_{i=1}^{n} X_i(e_i X_i)] \quad (3)$$

Xi represent mole fraction and $e_i X_i$ the standard chemical exergy of a substance calculated from equation (4). Where $g_{f,i}$ represent the standard molar free energy of formation and $e_j X_j$represent molar standard chemical exergy of constitute element [41, 42].

$$e_i^0 = g_{f,i} + \sum_{j=1}^{n,i} X_j(e_j X_j) \quad (4)$$

3.2.1 Exergy Performance Indicators

Exergy analysis is performed to find the system's thermodynamic performance. It comprises of system exergy efficiency, exergetic improvement potential, and irreversibility.

Irreversibility. Measures the amount of exergy destroyed in the unit process. In other words, it refers to the difference between the amount of exergy in and out of a unit process calculated from equation (5).

$$I = Ex_{destroyed} = \sum Ex_{in} - \sum Ex_{out} \quad (5)$$

In some process equipment such as distillation columns where condenser and reboiler play role in energy balance in addition to the feed and product streams, the (5) is modified to (6) for calculation of irreversibilities.

$$I = \sum (\dot{E}x_{feed} + (1 - \frac{T_o}{T_r})Q_r) - \sum (\dot{E}x_{Product} + \quad (1 - \frac{T_o}{T_c})Q_c) \quad (6)$$

Q_r and Q_c signify heat duty of reboiler and condenser and T_r and T_c denotes reboiler and condenser temperature.

Exergy efficiency. Measures the system's efficacy relative to system performance. In other words, it is the ratio of output to input exergy and calculated through equation (7) [7].

$$\varphi_{universal} = \frac{E_{out}}{E_{in}} \times 100 \quad (7)$$

Exergetic improvement potential. It's a measure of the amount of irreversibility which can be reduced in a unit process. It is denoted by 'I.P' and expressed in equation (9).

$$IP = (1 - \eta)(E_{in} - E_{out}) \quad (9)$$

3.3 Artificial Neural Network

Artificial neural networks (ANN) are a set of mathematical algorithms that imitate human brain functions to interpret data quantitatively through learning and training [43]. The ANN is composed of a network of neurons. Neurons receive inputs as variables and use their internal activation function to calculate outputs. Each input has a corresponding weight. As illustrated in Figure 6, the neuron's output will be computed using a nonlinear combination of its inputs (x_1, $x_{2...,}x_n$) and weights (w_1, w_2….,w_n). Through the process of learning, the synaptic weight is calculated. The learning aims to calibrate the network using a set of data for which both the input and

output values are known. In the Figure 6 'b' denotes the bais and 'f' activation function [44].

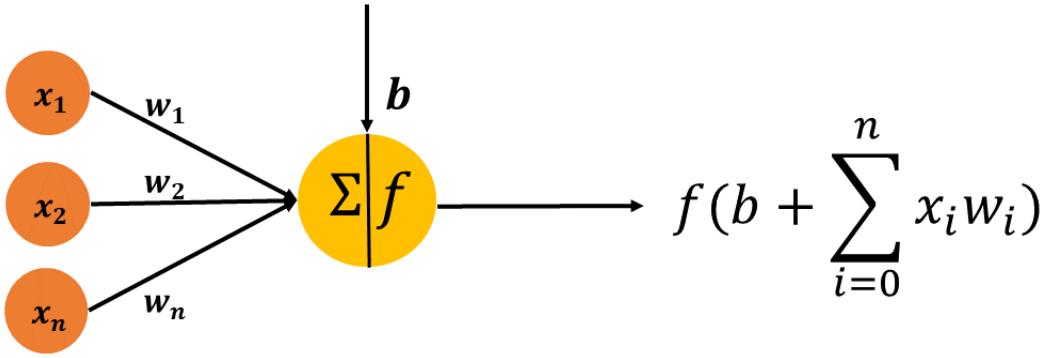

Figure 6: Neuron

A typical network has three main layers: input, hidden, and output to model complex and nonlinear functions as illustratied in Figure 7. The input layer receives information, feature, or data from external environments. The neurons in the hidden layers are accountable for extracting data regarding the system under examination. The output layer of neurons is responsible for creating and displaying the final network outputs, which result from the processing performed by the neurons in the preceding layer [45].

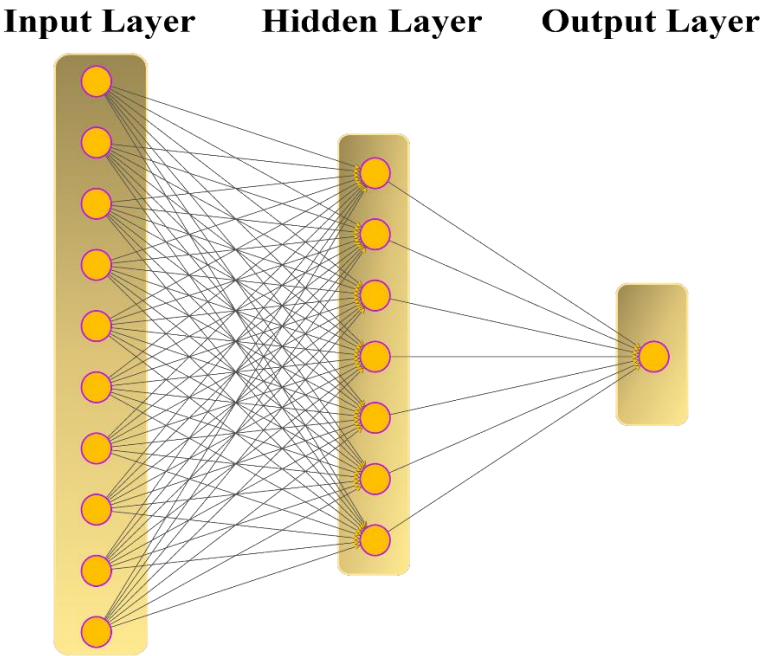

Figure 7: General ANN architecture

3.3.1 The Levenberg-Marquardt Method

The Levenberg-Marquardt method solves the nonlinear programing problem by reducing the sum of the squares errors between the model function and the data points through a sequence of well-chosen parameters update through gradient descent update and the Gauss-Newton update, as shown in equation (11).

$$[J^{\top}WJ + \lambda(J^{\top}WJ)\,]h_{|m} = J^{\top}W(y - \hat{y}) \qquad (11)$$

By changing the parameters in the steepest-descent direction, the sum of the squared errors is minimized in the gradient descent method. Assuming the least squares function is locally quadratic in the parameters and determining the minimum of this quadratic, the Gauss-Newton approach reduces the total of the squared errors. If the dumping parameter λ is small result in Gauss-Newton update, and if the λ is large results in a gradient descent update. The damping value λ is set to be big at the start so that the first updates are short steps in the steepest-descent direction. The λ minimized as the solution improved and the algorithm approached the Gauss-Newton method the solution moved toward a local minimum [46].

3.4 Genetic Algorithm

Genetic algorithm (G.A.) is a metaheuristic method used to solve optimization problems based on a natural selection process that intimate biological evolution (the survival of fitness). The algorithm continually revamps the population of individual solutions. At every step, the genetic algorithm generates children for the next generation. Selecting random individuals from the current population and using them as parents to find the best solution through fitness function. The algorithm stops if the objective function criteria are met. Otherwise, the evaluation process repeats until the population "evolves" toward the best solution through crossover, mutation, and selection probabilities, as shown in Figure 8 [47].

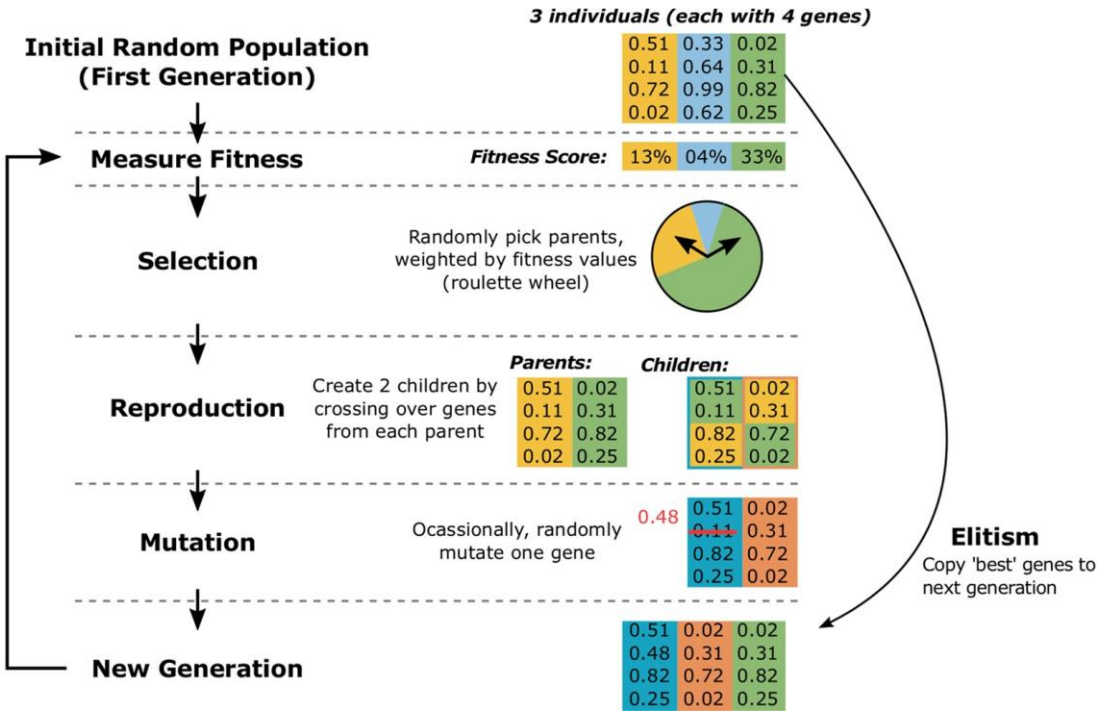

Figure 8: Schematic representation of Genetic Algorithm [48]

3.4.1 Genetic operators

The function of each genetic operator is as follows.

Population: An initial group of the population was generated randomly. Each possible solution is called a chromosome as shown in Table 1.

$$P = \{p_1, p_2, \dots, p_{pop\_size}\} \tag{12}$$

$$p_i = \left[p_{i_1}\ p_{i_2}\ \cdots\ p_{i_j}\ \cdots\ p_{i_{no-vars}}\right] \tag{13}$$

$$para^{\,j}_{min} \leq p_{i_j} \leq para^{\,j}_{max} \tag{14}$$

Table 1: Chromosomes

Chromosome 1	1101100100110110
Chromosome 2	1101111000011110

In equation 12 pop_size indicate the total size of population, and no_vars in equation 13 indicate the number of variables to be tuned, $para^{j}_{min}$ and $para^{j}_{max}$ are the minimum and maximum values parameter p_{i_j}.

Selection. Select a fraction of the existing population to breed a new population during every successive generation. Through fitness-based methods, individual

solutions are selected. The viability of each solution is evaluated, and the optimal one is selected. Roulette wheel, rank, stochastic universal sampling, and tournament are well-known selection methods [49].

In roulette wheel selection potential strings are mapped onto a wheel, and a fraction of the wheel is allocated based on their fitness value. Then the wheel is randomly rotated to select particular solutions that will take part in the formation of the next generation, as shown in Figure 9. Rank selection is upgraded from of roulette wheel. Individuals are evaluated based on their ranks rather than fitness value, giving every individual a chance to get selected.

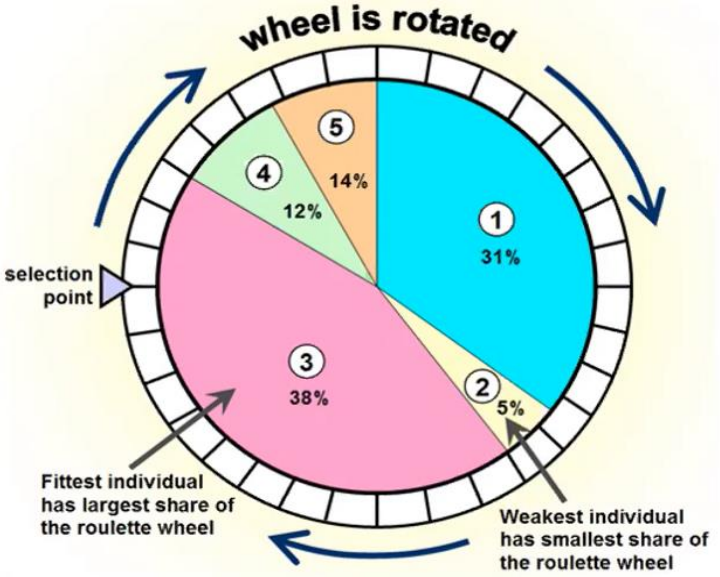

Figure 9: Roulette wheel selection

Stochastic universal sampling (SUS) selects a new individual at evenly spaced intervals through a random starting point from a list of individuals from a generation. The method gives equal opportunity to every individual to get selected.

Individuals are selected in tournament selection through a stochastic roulette wheel based on fitness value. The individual with better fitness is added to the pool of the next generation, as shown in Figure 10 [50].

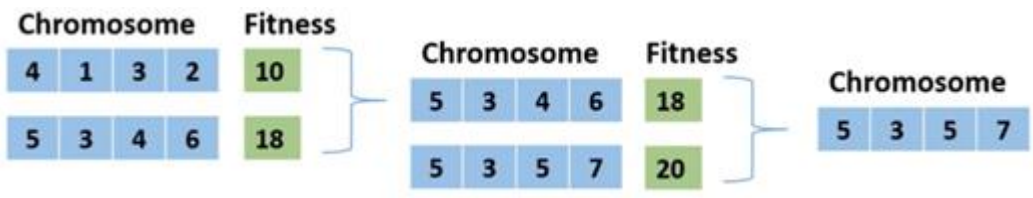

Figure 10: Tournament selection

Crossover. Produce childerns by combining the genetic information of two parents from the previous generation.

In a single-point crossover, a single random point is selected, and genetic information ahead of the point is swapped between the parents, as shown in Figure 11.

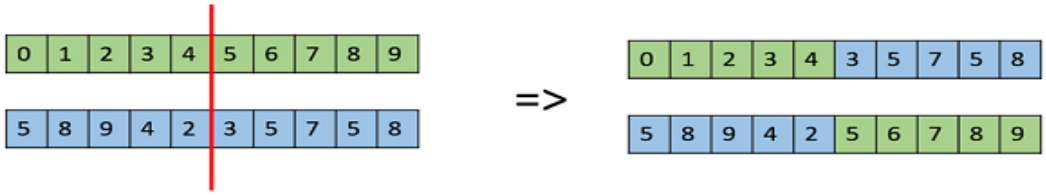

Figure 11: Single point crossover

In double point crossover, two points are randomly selected, and genetic information as per segment is swapped between the parents, as shown in Figure 12.

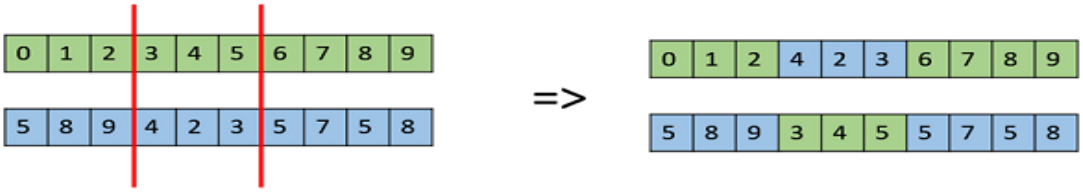

Figure 12: Double point crossover

In the uniform crossover, each gene in parents is treated separately. Arbitrary decisions are made on whether to swap the gene with another chromosome at the parallel spot, as shown in Figure 13 [51].

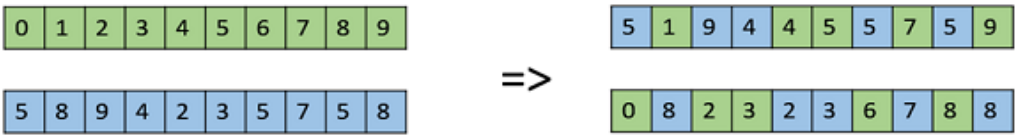

Figure 13: Uniform crossover

In the over scattered crossover a random chromosome is generated and genes are selected where the chromosome is 0 from second parent and where chromosome is 1 from fist parent. Then both are combined to form a child.

Mutation. Maintains the diversity of genes from one population to the next. The chromosomes' genes are changed during the mutation procedure. As a result, the characteristics of chromosomes acquired from their parents may be altered. The mutation procedure will produce three additional progeny [49].

3.5 Particle Swarm Optimization

Particle swarm optimization (PSO) is a population-based search algorithm inspired by the social behavior of birds in the swarm. A group of individuals called particles move in steps across the area. At every step, the algorithm assesses the objective function of each particle. The particle is drawn to the best place it has found so far or the best location any swarm member has found. After some steps, a swarm may congregate in one spot or a few spots or continue to move. After the evaluation, the algorithm decides a new velocity for each particle, and the algorithm revaluates as shown in Figure 14.

- The algorithm starts by generating initial particles and assigning them initial velocity.
- Find the best location and function value by assessing the objective function on every particle location.
- Select new particle velocity based on current velocity and best location of individual and neighbor particles.
- The algorithm repeats the whole process until objective criteria are met.

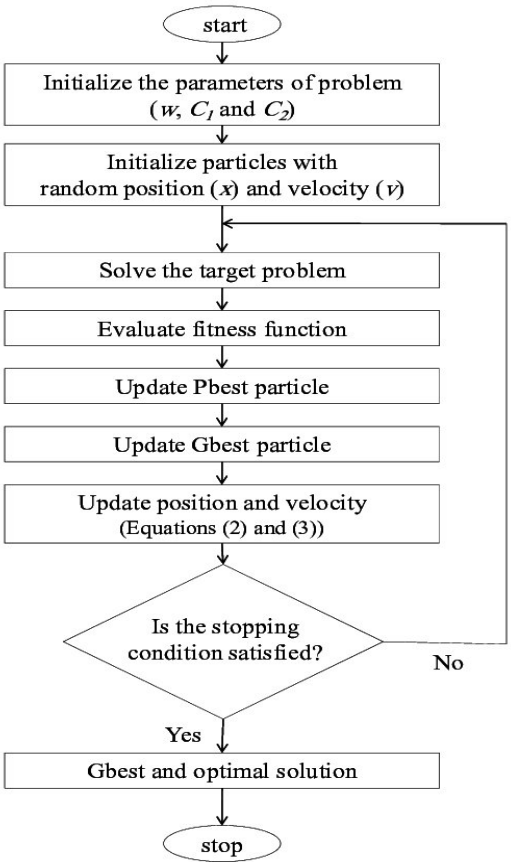

Figure 14: Work flow of particle swarm optimization [52]

3.6 Surrogate Model

The surrogate model, also known as the meta-model, is an analytical method to statistically relate the input and output behaviour of complex systems. Surrogate models are divided into two types based on approximation strategy (i) model-driven and (ii) data-driven or black box. Model-driven, also known as Reduce Order Model (ROM), reduces the computational cost by using order equations to approximate the original equations. However, the simulator source code is needed to apply this method which is mostly impossible when using commercial software. In a data-driven surrogate model is generated using input data and output response.

Following steps are used to develop a surrogate model.

1. The design space is conveniently sampled to identify the input parameters of data sets.
2. The simulator is run, or experiments are performed to calculate the outputs corresponding to the input parameters.
3. A surrogate model is selected and trained on training data (based on inputs and outputs).

4. Determined the model performance based on test data. If the model accuracy is unsatisfactory, the whole process repeats from step 1 [53].

3.7 Methodology

The methodology adopted for this study is summarized in Figure 15. The methodology comprises of four major steps briefly described below:

Phase I: Steady-state exergy analysis

Following assumptions were made during exergy analysis.

- Process units were modelled and evaluated as a steady-state flow system.
- Potential and kinetic exergies were ignored.
- Temperature and pressure values of 25^{o}C and 101.325 kPa were taken as reference conditions for exergy calculations.

The physical exergy of the process was calculated from the Aspen HYSYS V.10 property set. Then using the values of exergy the overall process and equipment irreversibility and exergy efficiency were calculated using equations (7) and (9). Exergetic improvement potential was of the process and equipment were calculated using the values of exergy destruction and efficiency from using equation (10).

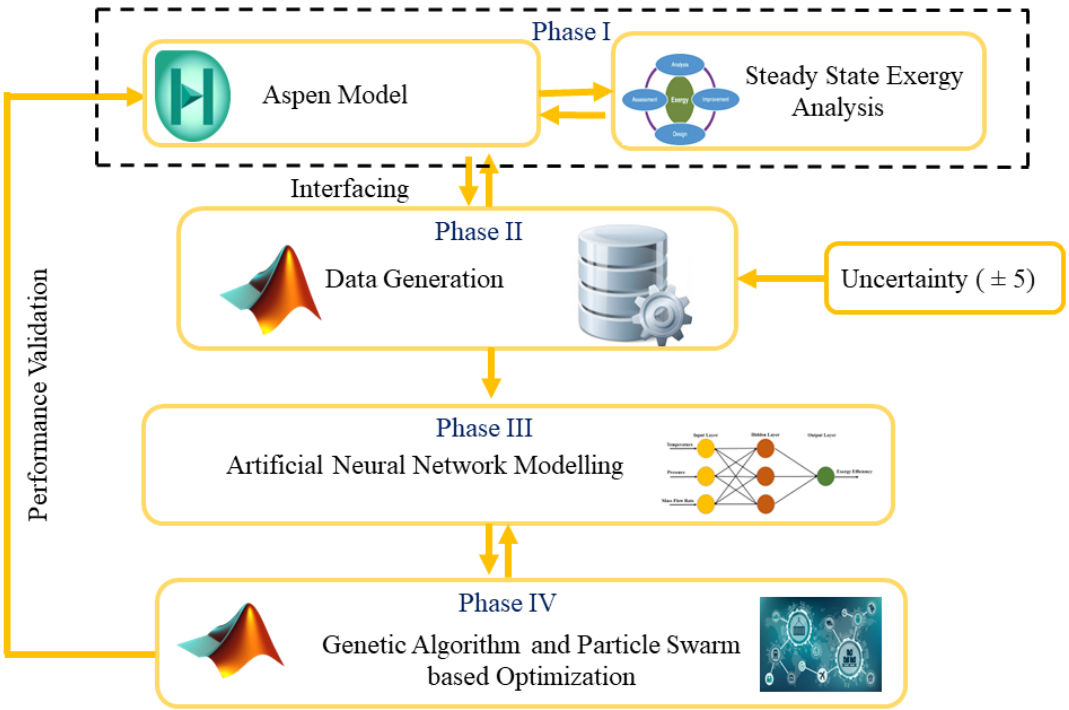

Figure 15: Methodology

Phase II: Data generation

Through COM server an interface was created between Aspen HYSYS and MATLAB software to generate data samples from the selected degree of freedom. The data sets were generated under random -5% and +5% uncertainty in process parameters. A total of 216 data samples were generated for integrated naphtha reforming and isomerization process and 200 for delayed coking process. Overall plant exergy efficiency was calculated using equation (7) for each data samples. Table 2 and Table 3 shows the data samples of delayed coking process and integrated naphtha reforming and isomerization process.

Table 2: Data samples of delayed coking process

Sr No.	Vacuum residue temperature (°C)	Vacuum residue mass flow rate (kg/hr)	Vacuum residue preassure (kPa)	Furnace temperature (°C)	Furnace pressure (kPa)
Data Sample 1	396.1421	190636.7	193.4237	465.1913	517.9294
Data Sample 2	398.3681	207818.1	200.1191	502.3121	497.5099
Data Sample 3	375.0012	189753.9	199.2195	483.1208	510.9882
Data Sample 4	392.4733	205410.8	199.2071	477.3437	494.8189
Data Sample 5	392.8507	203102	195.5205	500.2589	522.989
Data Sample 6	409.8662	195796.8	190.2075	486.6346	486.0043
Data Sample 7	407.4316	195570	202.6472	471.7224	531.0822
Data Sample 8	376.6606	197844.5	205.1548	511.2657	519.1155
Data Sample 9	382.5169	189874	200.5783	521.8001	494.8122
Data Sample 10	394.8897	187625.1	191.2403	512.2563	517.0897

Table 3: Data samples of integrated naphtha reforming and isomerization process

Process Conditions		Data Sample 1	Data Sample 2	Data Sample 3	Data Sample 4	Data Sample 5
Temperature (°C)	Isom Feed CatREF	20.81	19.88	19.95	19.89	19.74
	Reformer feed CatRef	19.25	19.76	19.70	19.21	19.22
	Off Gas	22.27	22.63	22.17	20.89	21.74
	DIST1 FEED	88.69	89.52	92.87	94.95	90.02
	DIST1BC Outlet	103.36	105.59	110.11	109.05	104.68
	T-100 Feed	206.63	204.55	201.27	213.25	197.37
	Total Fuel gas	14.30	15.38	14.49	14.47	14.93
	C3+C4	15.52	14.63	15.44	15.53	15.07
	ISOM2 Feed	160.76	163.50	153.82	167.61	158.64
	ProdSep Off-gas-	37.61	39.93	38.47	38.00	39.23
	Stabilizer Feed	130.30	121.65	125.28	128.17	118.96
	Raffinate-	37.85	36.85	34.66	35.95	35.24
Mass Flow rate (kg/hr)	Isom Feed CatREF	30997.5	29725.9	29147.4	30070.8	29103.1
	Reformer feed CatRef	52939.6	53045.4	52158.4	51234.8	53282.6
Pressure (kPa)	Isom Feed CatREF	3176.73	3243.77	3132.95	3070.87	3159.25
	Reformer feed CatRef	3067.90	3115.97	3027.81	2969.82	3003.1
	DIST1 FEED	214.61	203.69	214.58	205.83	208.55
	DIST1BC Outlet	833.00	831.12	877.62	828.88	872.14
	T-100 Feed	1940.5	1855.2	1948.5	1841.2	1954.6
	Isom Hydrogen Feed	2894.9	2888.2	2837.7	2936.5	3088.1
	Hot Feed	2447.2	2484.6	2655.4	2652.6	2546.6
	ProdSep Off-gas-	2371.3	2395.6	2217.1	2399.1	2282.2
	Stabilizer Feed	2331.56	2252.69	2361.51	2284.91	2274.83
	Raffinate-	609.96	602.47	623.71	620.66	609.29

Phase III: ANN Modeling

An ANN model was developed and validated using MATLAB 2022a. The modeling consists of model selection, training and validation.

- **Model selection:** A feed-forward neural network was selected with the Levenberg-Marquardt backpropagation (trainlm) training algorithm. Seventy percent (70%) of the data set is used for training; the rest of data samples are divided equally for model validation and testing. In the case of integrated naphtha reforming and isomerization, the ANN model has 33 input neurons, 5 hidden neurons, and 1 output neurons. Whereas in the case of delayed coking ANN model has 5 input neuron, 7 hidden neurons and 1 output neuron. The input neuron represents the uncertain process condition and output neuron represents the process exergy efficiency. Through trail and error the number of hidden layers and number of neurons in the hidden layer were selected. The ANN was set to run for 1000 epochs with a min gradient of 1e-7.

- **Training and validation:** The model is validated by following two criteria
  - Root mean-squared error (RMSE) and
  - Relation coefficient

RMSE is calculated from equation (15) and R from equation (16).

$$RMSE = \sqrt{\frac{1}{n}\sum_{i=0}^{n}(Y_i^{exp} - Y_i)^2} \tag{15}$$

$$R = 1 - \left[\frac{\sum_{i=0}^{n}\left(Y_i^{exp} - Y_i\right)}{\sum_{i}^{n}\left(Y_i^{exp} - Y_{avg}^{exp}\right)}\right] \tag{16}$$

Y_i^{exp} is the experimental value, Y_i is predicted data, and n represent a number of test samples. RMSE has a non-negative value, and a lower value is an indication of better model prediction performance. The coefficient of determination value ranges from 0 to 1, 0 being the value at which the output variable cannot be predicted from the regressor variable, and 1 means that the response variable is fully predictable from regressor variables.

Phase IV: Optimization The ANN model was used as a surrogate in a GA and PSO environment for optimization under uncertainty where exergy efficiency was the objective function. The GA and PSO found the optimal parameter with maximum exergy efficiency. The algorithm steps for GA are as follow

1) The algorithm start by generating a set of random populations of individual solution.
2) Performed fitness evaluation of each individual of population using surrogate model and rank them according to their fitness value.
3) Based on fitness value parent are selected to produce offspring using crossover operator.
4) Mutation operator are utilized to enhance the quality and maintain the genetic diversity of the proceding generation.
5) The algorithm stops if the objective function criteria are met; otherwise, steps 2-4 are repeated until optimal solution is reached.

The algorithm steps for PSO are as follows,

1) The algorithm starts by generating initial particles and assigning them initial velocity.
2) Surrogate model was used to evaluate the particle's position.
3) If the current position is better the previous one update the new personal best.
4) Assign the new personal best to global best.
5) Select new particle velocity based on current velocity and best location of individual and neighbor particles.
6) Repeat steps 2-5 until the stopping criterion is satisfied

The effectiveness of the proposed optimization was validated by running the Aspen HYSYS model on optimized results and finding the absolute error.

Chapter 4

Results and Discussion

Section 4.1 and 4.2 presents the steady-state exergy analysis of integrated naphtha reforming, isomerization, and delayed coking processes. Section 4.3 presents data-based modeling and optimization of exergy efficiency.

4.1 Steady state exergy analysis of integrated naphtha reforming and isomerization process

4.1.1 Stream wise exergy analysis

The operating conditions and exergy calculations of process streams are presented in Table 4 and Table 5. Some streams have zero exergies values in Table 4 and Table 5 because they are at the reference temperature and pressure conditions. Exergies of process streams were calculated in Aspen HYSYS environment. In naphtha reforming unit, Hp-in has the highest exergy of 4073.14 kW followed by platformate, Hp-out, T-100 Feed and Net hydrogen with the exergy value of 2194.22 kW, 1762.93 kW, 1174.68 kW and 855.90 kW respectively. While Cw-in, platformer Bypass, isom feed to tank, Lp isom feed, and Hypos have the lowest exergy value of' zero'. Whereas in isomerization process HP-In has the highest exergy of 2741.44 kW followed by Isomerate ISOM1, Hot Feed, HP-Out and Isomerate ISOM101 with the exergy value of 1793.44 kW, 1387.72 kW, 1267.78 kW and 1202.86 kW respectively. While CW2-in and Ben has the lowest exergy of '0' followed by NC6, Hypos, and others with exergy value of 0.09 kW, 0.09 kW and 0.15 kW.

4.1.2 Equipment level exergy destruction (Irreversibility)

Process irreversibility determines the amount of exergy destroyed in a unit operation or process. Irreversibility in any unit operation or process is caused due to

- Spontaneous chemical reaction
- Transfer of heat at finite temperature differences
- Dissipation of work to heat by fluid friction or solid
- Unrestricted expansion or temperature equalization in a mixing [7, 54]

Table 6 presents exergy destruction of individual unit operations of integrated naphtha reforming and isomerization units. Figure 16 depicts each unit operation's contribution to the overall plant's irreversibility. The reformer section contributes 57.30% to the total irreversibility of the overall unit. The reformer reaction section consists of three furnaces and three rectors. During fuel combustion, 30% of the total fuel exergy content was lost in the furnace, while only 70% of chemical exergy was converted into physical. Most of this physical exergy was lost due to the finite temperature difference between the sink and the source. While in reactors, irreversibility is generated due to endothermic reaction.

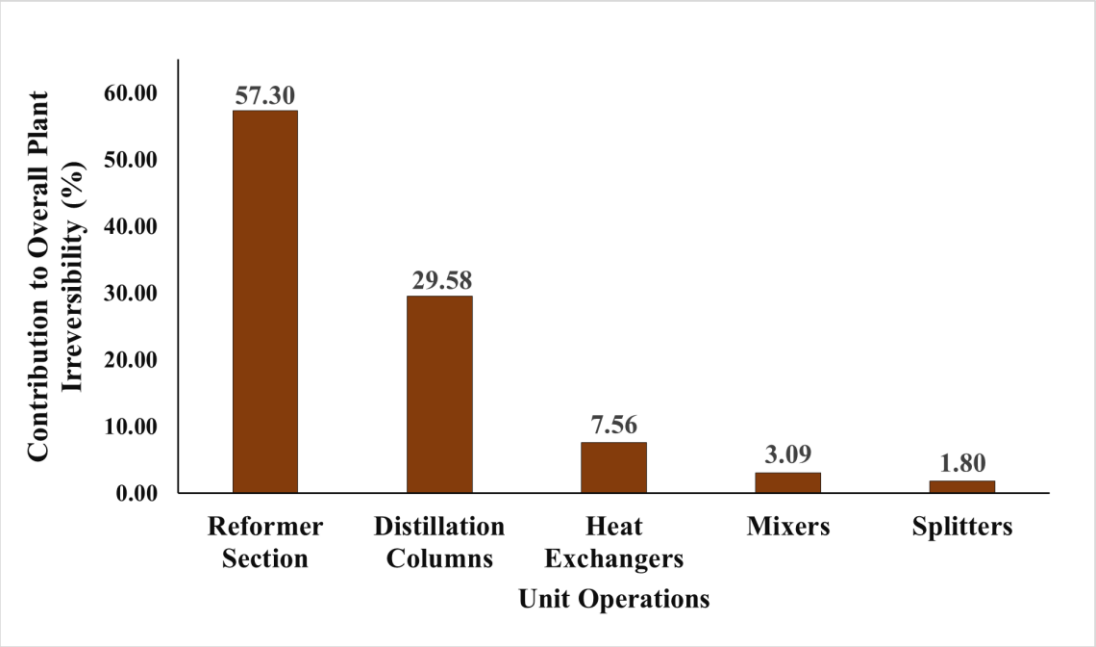

Figure 16: Units operations contributing to irreversibility of integrated naphtha and isomerization process

Followed by distillation columns (DIST1, T-100, Stabilizer) contributing 29.58% because of poor remixing and pressure distribution and inadequate heat and mass transfer between the vapor and liquid phases [55, 56]. Similarly, heat exchangers (DIST1, DIST1BC, E-100, E101, E102) contribute 7.56% due to the finite temperature difference between the hot and cold streams [57]. In the case of mixers and tees, many of them are 100% exergy efficient, while some contribute 3.09% to plant irreversibility. Splitters contribute only 1.8%. Isomerization reactors (ISOM100, ISOM101) were another major contributor. Due to the limitation of equilibrium on the reaction. The reaction is exothermic but needs to occur at a low temperature.

Table 4: Naphtha reforming unit streams process conditions and exergy values

Streams Names	Mass flowrate (kg/hr)	Temperature (ºC)	Pressure (kpa)	Exergy (kW)
Isom Feed CatREF*	29708.25	20.00	3101.33	41.36
Reformer feed CatRef*	52010.00	20.00	3101.33	67.57
1	29708.43	20.00	3101.33	36.77
2	52010.00	20.00	3101.33	60.25
Combined Naphtha	81718.49	21.98	3101.33	95.62
Off Gas*	89.21	21.82	3101.33	1.00
Bottoms	81629.27	21.82	3101.33	95.58
LP-In	5565.00	125.00	101.33	778.20
LP-out	5565.00	99.96	101.33	92.74
DIST1 FEED*	81629.27	92.41	211.33	338.79
DIST1 Liquids	29502.28	32.08	108.33	1.53
DIST1 Bottoms	52126.99	145.22	204.33	647.19
Cw-IN	237343.16	25.00	101.33	0.00
CW-OUT	237343.16	29.86	101.33	11.21
DIST1BC Outlet*	52126.99	105.70	861.33	309.72
platformer Bypass	0.00	105.70	861.33	0.00
Platformer Feed	52126.99	105.70	861.33	309.72
Net Hydrogen	4611.64	28.00	350.00	855.90
Unstab platfomate	47463.15	30.00	825.00	13.04
Hp-in	10319.28	670.00	1200.00	4073.14
Hp-out	10319.28	180.04	1200.00	1762.93
T-100 Feed*	47463.15	205.67	1901.33	1174.68
T-100 off Gas	276.39	206.37	1879.33	14.66
T-100 Liquid	6129.96	206.37	1879.33	173.29
Platfomate	41056.79	292.60	1891.00	2194.23
Net Hydrogen Product	3871.64	28.00	350.00	720.09
To issom	740.00	28.00	350.00	135.82
To isom Input	740.00	28.00	350.00	135.82
Isom Hydrogen Feed*	740.00	38.36	2961.00	368.85
Isom feed to tank	0.00	32.08	108.33	0.00
isom feed	29502.28	32.08	108.33	1.53
Lp isom feed	0.00	20.00	3101.33	0.00
Isom Fresh Feed	29502.28	32.08	108.33	1.53
pure comp	27887.01	32.08	108.33	1.44
Hy pos	1615.27	32.08	108.33	0.09
Isom off gas	2437.64	41.88	1300.00	207.21
Isomerate	27625.85	54.10	621.33	28.25
Light end	8933.21	126.94	1300.00	341.45
Total Fuel gas*	320.29	15.00	1601.33	144.04
C3+C4*	8612.92	15.00	1601.00	19.58
Gasoline product	68682.64	164.09	621.33	1634.25

* These stream parameters used in ANN training

Table 5: Isomerization unit streams process conditions and exergy values

Streams Name	Mass flowrate (kg/hr)	Temperature (ºC)	Pressure (kpa)	Exergy (kW)
Isom Hydrogen Feed*	517.01	38.18	2961.00	366.91
Pure Comps	27886.82	32.08	108.33	1.49
Hypos	1615.27	32.08	108.33	0.09
Isom Fresh Feed	29502.09	32.01	108.33	1.55
Extract Recycle	3389.61	92.40	3441.33	20.91
HC Feed	32891.70	38.98	108.33	6.55
Cold Feed	33408.71	16.73	108.33	17.14
HP-In	10000.00	300.00	500.00	2741.44
HP-OUT	10000.00	151.68	500.00	1267.78
Hot Feed*	33408.71	162.90	2550.00	1387.72
Isomerate ISOM1	33455.02	196.00	2549.89	1793.44
CW2-in	272198.88	25.00	101.33	0.00
CW2-OUT	272198.88	29.53	101.33	236.89
ISOM2 Feed*	33455.02	161.00	2549.89	1178.46
Isomerate ISOM101	33455.02	161.94	2549.81	1202.86
ProdSep Off-gas-*	609.10	38.94	2297.00	147.52
Isomerate to Stab heater	32845.92	38.94	2297.00	73.79
MP-IN	3670.03	250.00	200.00	835.15
MP-OUT	3670.03	120.94	200.00	262.60
Stabilizer Feed*	32845.92	124.44	2287.00	400.85
Stabilizer Off-gas	1831.71	49.70	1300.00	85.17
Stabilized Isomerate	31014.21	153.92	1465.00	531.70
Isom Off Gas	2440.81	40.70	1300.00	207.89
Isomerate to Storage	3642.41	153.92	1465.00	62.46
CSPLIT Feed	27371.80	153.92	1465.00	469.24
Raffinate-*	23983.34	36.20	621.33	8.80
Isomerate pre-RON	27625.75	54.31	621.33	30.08
Isomerate-	27625.75	54.31	621.33	30.08
Isomerate	27625.75	54.31	621.33	30.08
IC4*	419.00	25.00	621.33	7.47
IC5*	9525.63	25.00	621.33	2.43
IC6*	13125.97	25.00	621.33	3.00
NC4*	409.31	25.00	621.33	4.88
NC5	1689.59	25.00	621.33	0.44
NC6*	377.57	25.00	621.33	0.09
BEN*	0.26	25.00	621.33	0.00
Other*	731.77	25.00	621.33	0.15

* These stream parameters used in ANN training

Table 6: Exergy destruction of individual unit operation of integrated naphtha and isomerization process

Naphtha reforming		Isomerization	
Unit operation	**Exergy destruction (kW)**	**Unit Operation**	**Exergy destruction (kW)**
CUT-100	4.59	Mix-100	0.0269
CUT-101	7.32	HC Mixer	15.92
Mix-100	1.4	Feed Mixer	362.59
CSPLIT1	0	E-100	97.04
DIST1	439.41	Isom100*	-365.297
DIST1-COLUMN	8171.59	E-101	332.9
DIST1BC	325.19	Isom101*	-23.56
TEE-100	0	Product Seperator	998.31
REFORMER-100	21724.72	Stabalizer feed heater	243.03
E-100	1151.08	Stablizer	773.67
T-100	1459.01	Off gas mixer	30.6
TEE-101	0	Isomerate split	0
MIX-105	0	Csplit	448.2
X-100	0.01	Isomerate mix	41.99
MIX-104	57.13	Manipulator	0
CSPLIT2	177.2	Valve	0
MIX-106	596.87	X-100	14.16
TEE-102	0		

Isom100 and Isom101 are fixed bed reactors with negative exergy destruction because chemical exergy is not included.

4.1.3 Plant level exergy destruction (irreversibility)

Figure 17 depicts visual exergy accounting of the integrated naphtha reforming and isomerization process in the form of a Grassman diagram. The thickness of the lines shows the amount of exergy the stream takes in or out from the plant. As depicted in Figure 17, furnace and reboiler duties were the main sources of exergy in the plant, with an exergy value of 31842.0 kW and 15151.8 kW and also the main source of exergy destruction. A total of 70723.63 kw exergy entered the plant and 35768.08 kW came out. The plant has overall exergy destruction of 34955.55 kW. The exergy destruction of naphtha reforming and isomerization units were 32041.77 kW and 2913.78 kW, respectively. The exergy destruction of naphtha reforming and isomerization units contributes 91.66% and 8.33% to overall plant exergy destruction.

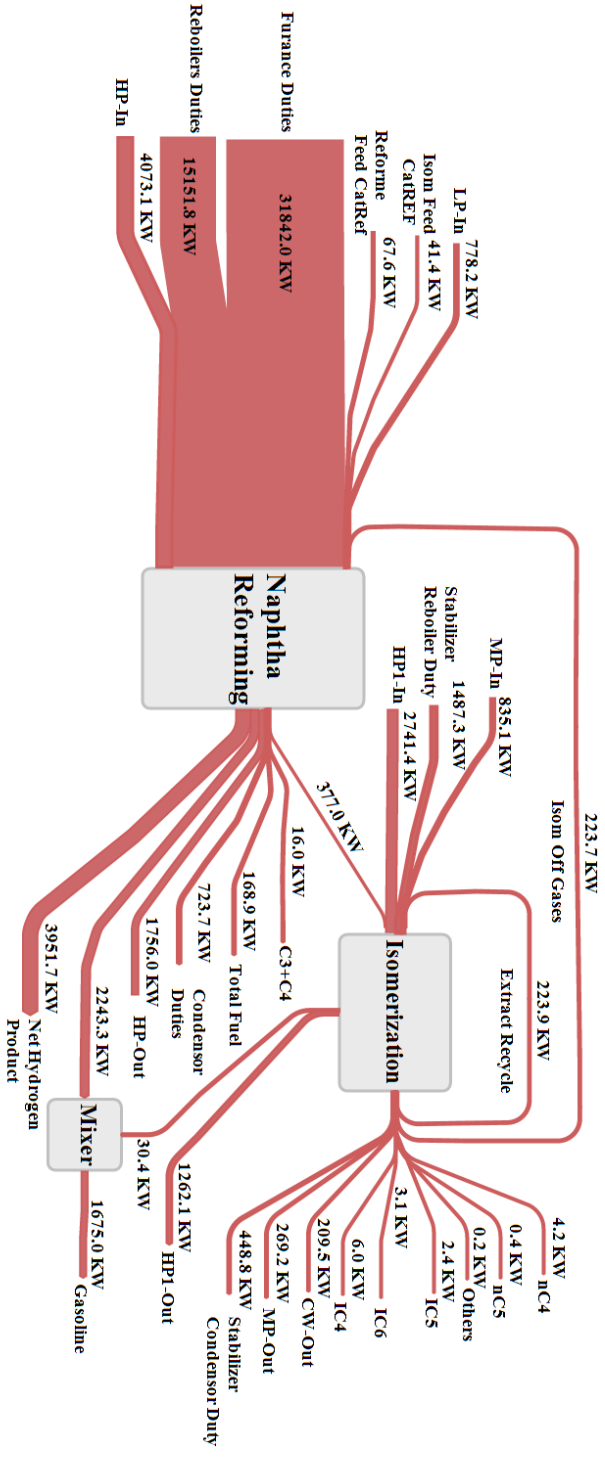

Figure 17: Grassman Diagram of Integrated Process of Naphtha Reforming and Isomerization

4.1.4 Exergy efficiency

Exergy efficiency measures the system's efficacy relative to system performance. Figure 18 shows the exergy efficiency of each reactive unit. The overall exergy efficiency of a plant was 50.57%. The exergy efficiency of naphtha reforming and

isomerization units were 44.61% and 77.38%, respectively. Table 7 presents the exergy efficiency of individual units of naphtha reforming and isomerization units calculated from equation (10). In naphtha reforming, DIST1-column was least efficient followed by reformer-100 and CSPLIT2 with exergy efficiency of 30.13%, 37.38% and 47.92% respectively. While TEE-100, TEE-101, TEE-103 and MIX-105 has the highest exergy efficiency of 100%. Whereas in isomerization, feed mixer, Csplit and Psep were least efficient with an exergy efficiency of 4.59%, 6.33%, and 18.40%, respectively. While Valve, Maniupltor and isomerate split has the highest exergy efficiency of 100%.

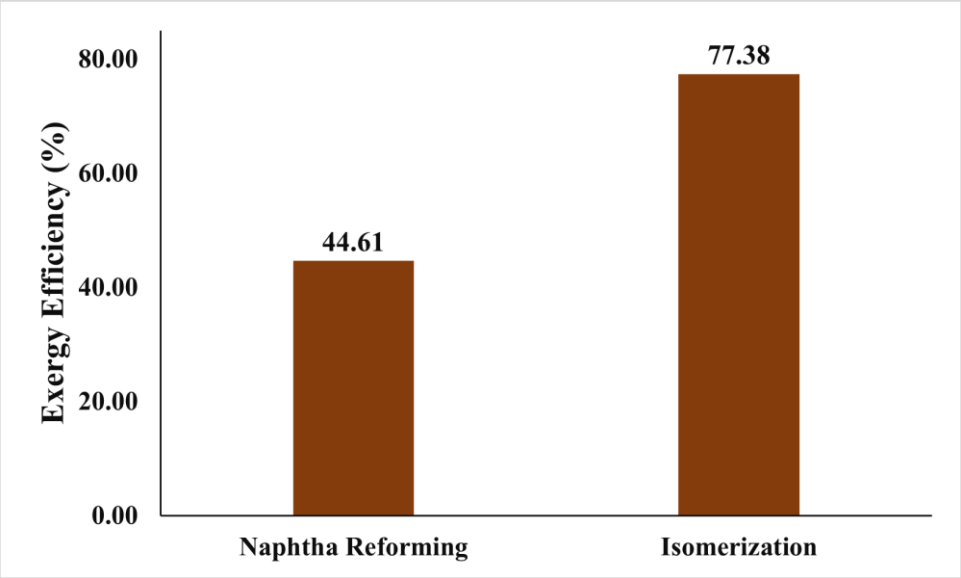

Figure 18: Exergy efficiency of reactive units of integrated naphtha and isomerization process

Table 7: Exergy efficiency and improvement potential of individual unit operations of integrated naphtha and isomerization process

Naphtha reforming		Isomerization	
Unit Operations	**Exergy Efficiency (%)**	**Unit Operations**	**Exergy Efficiency (%)**
CUT-100	88.90	Mix-100	98.33
CUT-101	89.17	HC Mixer	29.14
Mix-100	98.56	Feed Mixer	4.59
CSPLIT1	99.88	E-100	96.26
DIST1	49.39	Isom100	129.24
DIST1-COLUMN	30.13	E-101	78.92
DIST1BC	49.59	Isom101	102.07
TEE-100	100.00	PSEP	18.40
REFORMER-100	37.38	Stab feed heater	72.99
E-100	71.89	Stabilizer	59.83
T-100	70.98	off gas mixer	89.34
TEE-101	100.00	isomerate split	100.00
MIX-105	100.00	Csplit	6.33
X-100	99.83	isomerate mix	42.21
MIX-104	86.19	Manipulator	100.00
CSPLIT2	47.92	Valve	100.00
MIX-106	73.53	X-100	61.33
TEE-102	100.00		

4.1.5 Exergetic improvement potential

Table 8 presents the exergetic improvement potential of individual unit operation of naphtha reforming and isomerization unit calculated from equation (11). The overall process has exergetic improvement potential of 17276.98 kW. Figure 19 shows exegetic improvement potential of each unit in comparison to their irreversibility. The exergetic improvement potential of the naphtha reforming and isomerization unit was 17749.25 kW and 659.15 kW, respectively. In naphtha reforming, reformer-100 and DIST1-column have the highest improvement potential of 12541.91 kW and 5719.30 kW, respectively. Whereas in isomerization, Psep and csplit, have the highest improvement potential of 800.96 kW and 411.69 kW respectively.

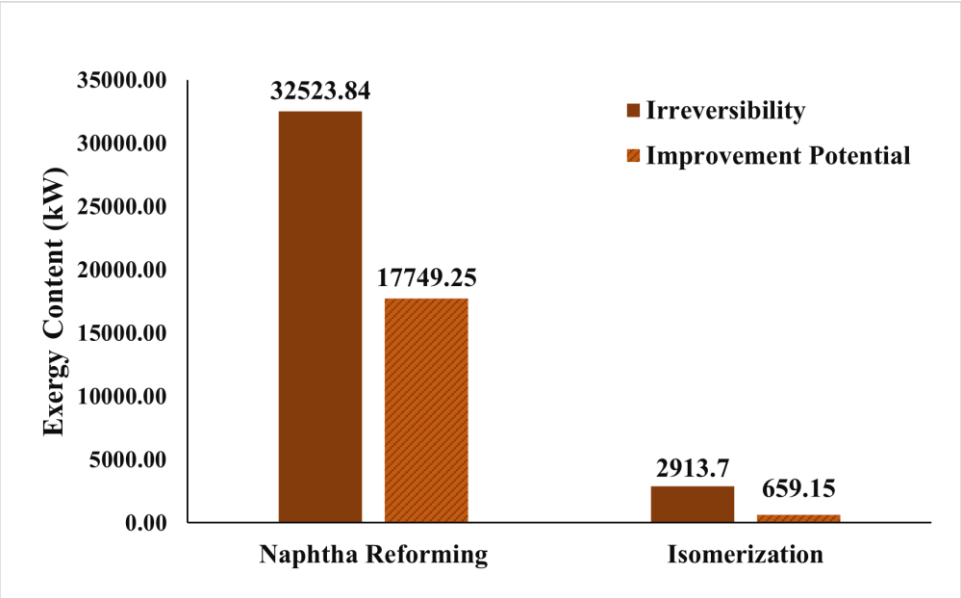

Figure 19: Exergetic improvement potential of reactive units compared to their irreversibility of integrated naphtha and isomerization process

Figure 20 shows exergetic improvement potential of the unit's operation. The exergetic improvement potential of the reaction section, distillation columns, heat exchangers, mixers, and splitters was 5802.70 kW, 631.49 kW, 351.92 kW, and 421.48 kW, respectively.

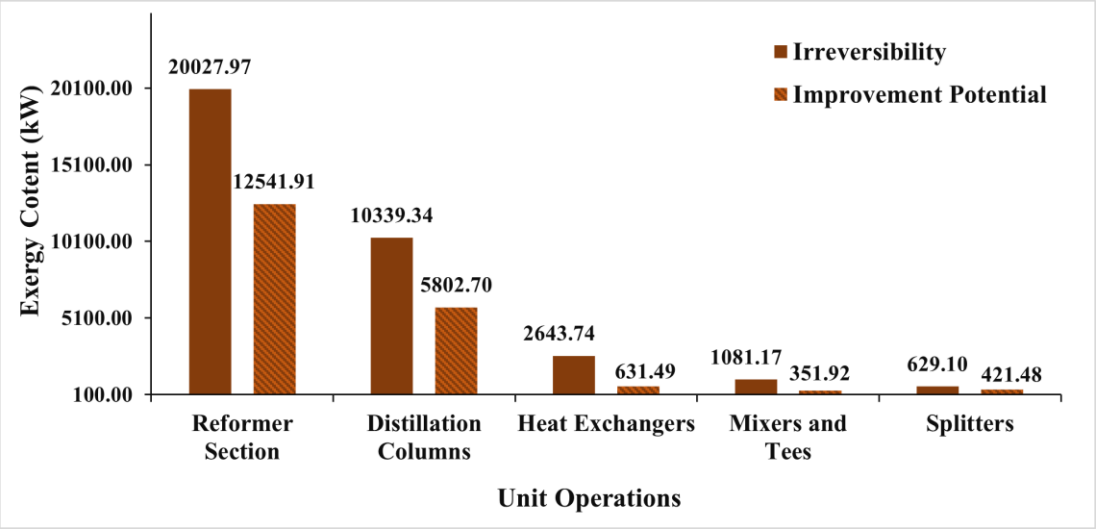

Figure 20: Exergetic improvement potential of unit operations compared to their irreversibility

Following changings are recommended to increase the exergy efficiency and reduce the exergy losses. For distillation columns, remixing losses can be mitigated by selecting the appropriate feed location. Effective internal flow arrangement and heat

exchanger design can control the pressure and heat losses while the mass transfer losses can be minimized by secondary reflux [55, 58]. In addition, replacing conventional columns with internally heat integrated columns, dividing wall columns, and reactive distillation columns can reduce substantial exergy losses [59]. The exergy efficiency for heat exchangers can be enhanced by decreasing the temperature difference between hot and cold media. As for the mixer, the exergy losses can decrease by bringing the stream's temperature close to each before mixing [60]. For reforming reactors, replacing conventional bed reactors with membrane bed reactors or applying advanced control systems can enhance exergy efficiency [59, 61]. And furnaces exergy losses can be mitigated by heat integration. Before implementing these exergy solutions, it is essential to estimate their economic effect through exergoeconomics studies.

Table 8: Improvement Potential of of individual unit operations of integrated naphtha and isomerization process

Naphtha reforming		**Isomerization**	
Unit Operations	**Improvement Potential (kW)**	**Unit Operations**	**Improvement Potential (kW)**
CUT-100	0.51	Mix-100	0.00
CUT-101	0.79	HC Mixer	11.28
Mix-100	0.02	Feed Mixer	339.97
CSPLIT1	0.00	E-100	3.85
DIST1	223.83	Isom100	118.62
DIST1-COLUMN	5719.30	E-101	79.71
DIST1BC	164.48	Isom101	0.51
TEE-100	0.00	PSEP	800.96
REFORMER-100	12541.91	Stab feed heater	66.30
E-100	322.85	Stabilizer	299.80
T-100	408.42	off gas mixer	2.64
TEE-101	0.00	isomerate split	0.00
MIX-105	0.00	Csplit	411.69
X-100	0.00	isomerate mix	23.80
MIX-104	7.55	Manipulator	0.00
CSPLIT2	92.61	Valve	0.00
MIX-106	155.69	X-100	4.50
TEE-102	0.00		

4.2 Steady State Exergy Analysis of Delayed Cocker Process

4.2.1 Stream level exergy analysis

The operating conditions and exergy calculations of process streams are presented in Table 9. Physical exergies of process streams were calculated in Aspen HYSYS environments. Coker feed had the highest exergy value of 22601.06 kw followed by Coker offgas and Recycle to column with the exergy value of 21658.03 kW while LPG, Reflux and Naphtha has the least exergy value of 0, 232.77 and 290.62 kW, respectively.

Table 9: Delayed cocking unit streams process conditions and exergy values.

Stream Name	Temperature (°C)	Pressure (kPa)	Mass flowrate (kg/hr)	Exergy (kW)
Vacuum Residue	395.00	200.00	200000.00	18034.76
Recycle to column	458.87	200.00	169042.27	21658.02
Naphtha	165.74	146.90	20000.00	290.62
LGO	242.28	172.76	10886.42	334.52
HGO	350.00	188.28	70509.06	4743.91
Coker feed	417.34	190.00	230996.44	22601.06
Coker Offgas	458.87	200.00	169043.82	21658.03
LPG	65.00	140.00	0.00	0.00
Reflux	65.00	140.00	169841.02	232.77
Fuel Gas	65.00	140.00	36650.34	352.02

Table 10: Exergy destruction, exergy efficiency, and improvement potential of delayed coking unit

Unit Operation	Exergy destruction (kW)	Exergy efficiency (%)	Improvement potential (kW)
Delayed Coker	9144.408	70.31272	2714.727
Furnace	5344.066	85.21554	790.0913
Column	14715.55	64.80535	5179.086
Recycle	0	99.99996	0

4.2.2 Plant and equipment level exergy destruction (irreversibility)

Table 10 depicts the exergy destruction, efficiency, and improvement potential of individual unit operation of the delayed cocker process calculated from equations (7), (9), and (10). Figure 21; depicts visual exergy accounting of the delayed cocker process in the form of a Grassman diagram. The thickness of the lines showed the amount of exergy coming in and out from the process. A total of 130418.9 kW exergy

entered the plant, and 101214.8 kW came out. The plant has overall exergy destruction of 29204.035 kW. The distillation column (T-100) contributes 50.039% to overall plant exergy destruction because of poor remixing, pressure distribution, and inadequate heat and mass transfer between the vapour and liquid phases [55, 56]. Coker drums and furnaces contributed 31.31% and 18.30%, respectively, as depicted in Figure 22. In the furnace, the cracking reaction intrinsic irreversibility contributes most to the unavoidable losses. During fuel combustion, 30% of the total fuel exergy content was lost, while only 70% of chemical exergy was converted into physical. Most of this physical exergy was lost due to the high-temperature gradient along the furnace tubes, sharp pressure drops, and the finite temperature difference between the heat media and cold stream [60, 62].

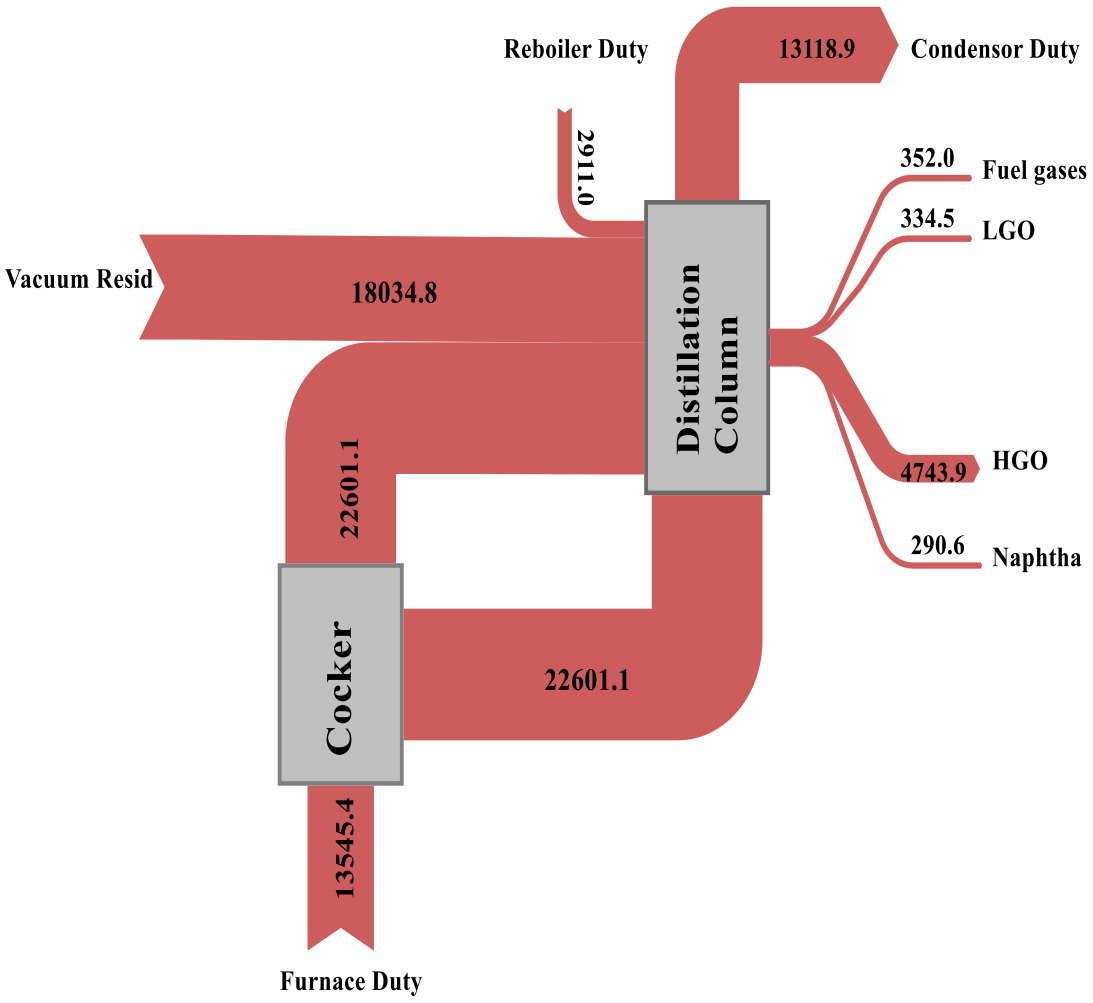

Figure 21: Grassman diagram of delayed cocker

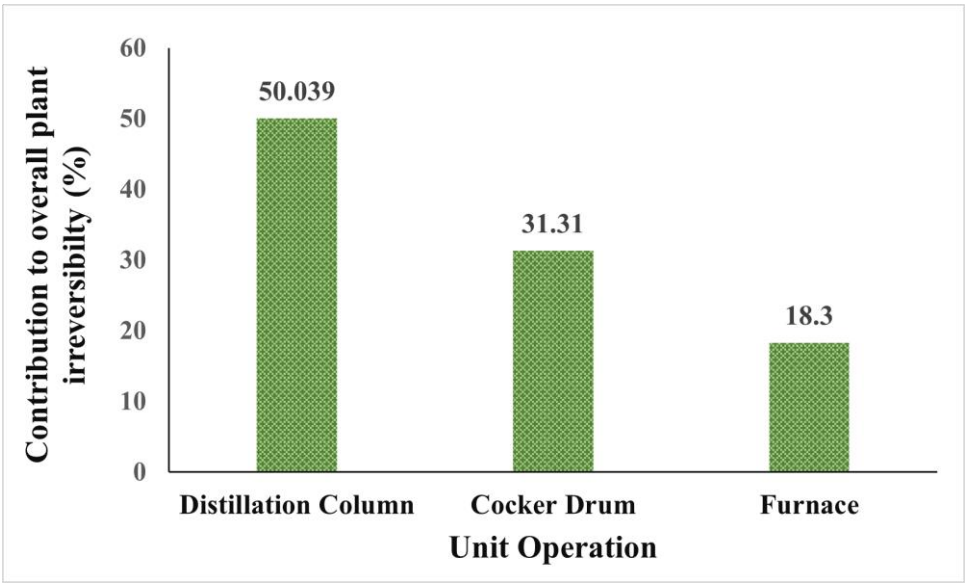

Figure 22: Units contributing to irreversibility

4.2.3 Exergy efficiency

Table 10 shows the exergy efficiency of each unit. The overall exergy efficiency of a plant was 77.61%. The exergy efficiency of the distillation column delayed cocker and furnace units were 64.81%, 70.31%, and 85.22%, respectively.

4.2.4 Exergetic improvement potential

The overall process has an exergetic improvement potential of 6539.51 kW. Figure 23 shows the exegetic improvementt potential of each unit in comparison to its irreversibility. The exergetic improvement potential of the distillation column delayed cocker and furnace units were 5179.1 kW, 2714.7 kW, and 790.09 kW, respectively. The following changings are recommended to increase the exergy efficiency and reduce the exergy losses. Increasing the number of tubes and shortening their length in the furnace can reduce significant temperature differences along the tube. Enhancing the heat distribution inside the furnace is another modification to minimize irreversibility achieved by floor firing or a combination of floor firing and sidewall. Preheating feed through an economizer can reduce the temperature difference between heat media and cold stream. For distillation columns, remixing losses can be mitigated by selecting the appropriate feed location. Effective internal flow arrangement and heat exchanger design can control the pressure and heat losses while the mass transfer losses can be minimized by secondary reflux [55, 58]. Furthermore, replacing conventional columns with internally heat-integrated and reactive distillation columns can reduce substantial

exergy losses [59]. Before implementing these exergy solutions, it is essential to estimate their economic effect through exergoeconomics studies.

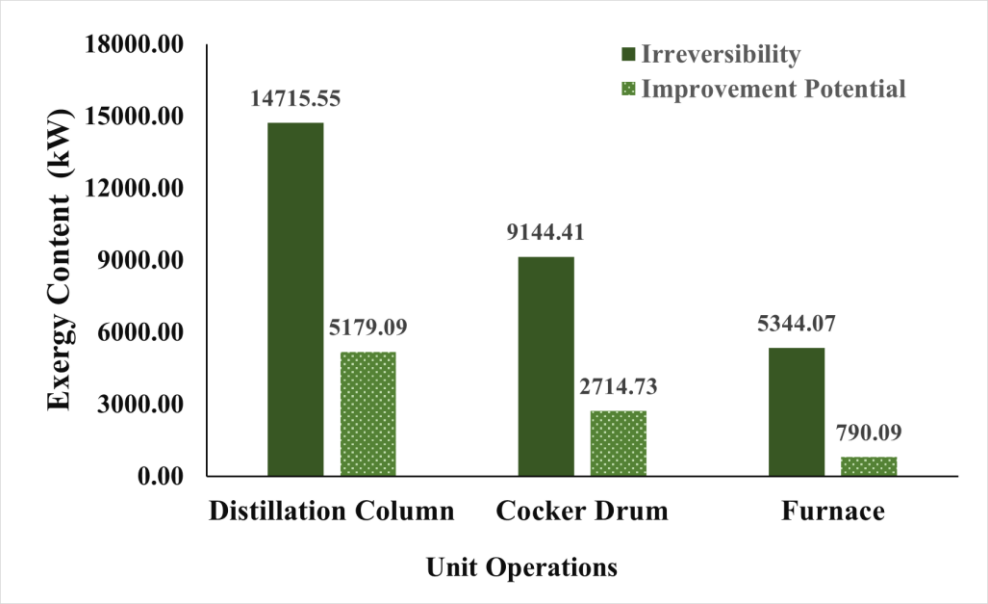

Figure 23: Exergetic improvement potential of reactive units compared to their irreversibility

4.3 Data based modeling and optimization

In the previous section, we performed a steady-state exergy analysis. While In this section, we incorporate uncertainty in process parameters and generate different data samples where input was uncertainty in process parameters and output was exergy efficiency. Then we developed ANN model on generated data samples and used it as a surrogate in GA and PSO environments to optimize the uncertain process condition. Optimization algorithms aimed to overcome the artificially inserted uncertainty to achieve maximum exergy efficiency. The reason behind the implementation of two optimization algorithms was to cross-check their performance.

4.3.1 ANN training, validation, and prediction of exergy efficiency of integrated naphtha reforming and isomerization process

The ANN model was developed in MATLAB 2022a. The uncertainty of +5% and -5% were inserted in the 33 uncertain conditions given in Table 3 and Table 4. A total of 216 data samples were generated; 154 were used for model training, 27 for validation, and 35 for model testing. ANN has trained with the Levenberg-Marquardt backpropagation (trainlm) training algorithm while network behavior was controlled through the Tansig activation function. ANN model with one, two, and three hidden

layers with varying numbers of neurons were iteratively tested to validate the best network architecture. The RMSE was used to quantify the performance of the model architecture. The model with one hidden layer and 5 neurons in the hidden layer were found to be the best design with the least RMSE. In addition to the built-in distribution of samples by ANN into training and testing, 35 data samples (test samples) were kept unknown to the model to asses its generalization as shown in Figure 24. The ANN model had an R of 0.97432 and an RMSE of 0.0348 for exergy efficiency.

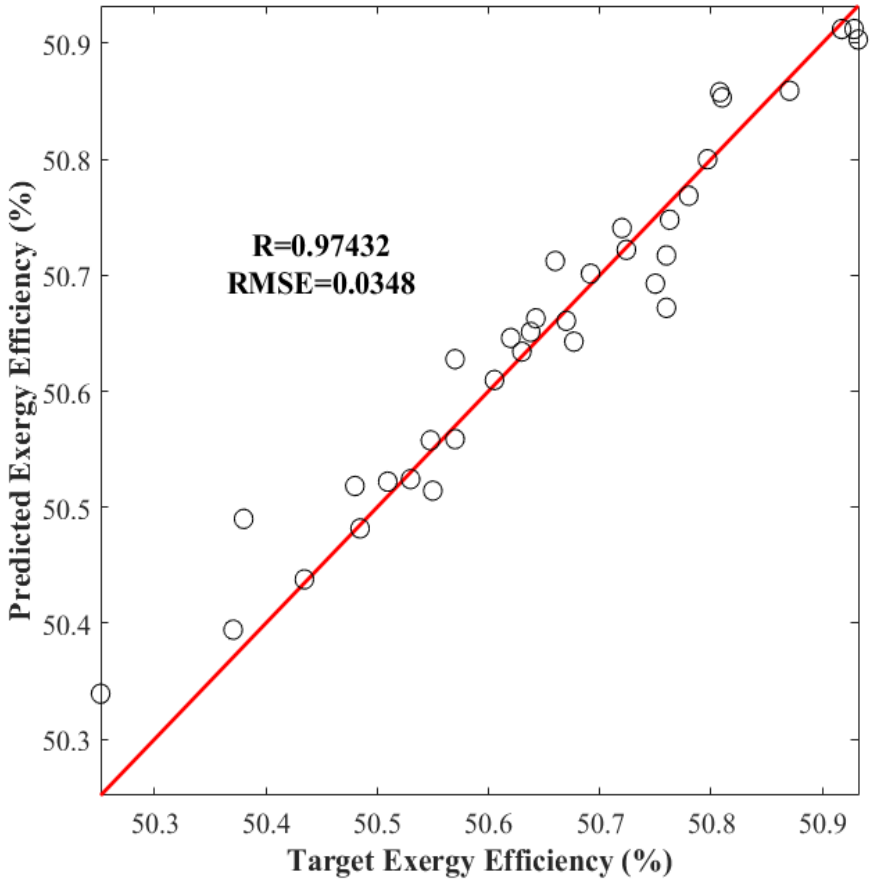

Figure 24: Predicted vs actual exergy efficiency of integrated naphtha reforming and isomerization process

4.3.2 ANN training, validation and prediction of exergy efficiency of delayed coking process

The ANN model was developed in MATLAB 2022a. The uncertainty of +5% and -5% were inserted in the vacuum residue temperature, furnace temperature, vacuum residue mass flow rate, furnace pressure, and vacuum residue pressure. ANN trained with the Levenberg-Marquardt backpropagation (trainlm) training algorithm, network behaviour control through Tansig sigmoid activation. From the 200 data samples

generated, 140 were randomly taken for model training, and 60 data sets for model validation and testing. ANN model with one and two hidden layers with varying numbers of neurons was iteratively tested to validate the best network architecture. The RMSE was used to quantify the performance of the model architecture. The model with one hidden layer and seven neurons in the hidden layer was the best design with the least RMSE. In addition to the built-in distribution of samples by ANN into training and testing, 30 data samples (test samples) were kept unknown to the model to asses its generalization as shown in Figure 25. The ANN model had R of 0.98198 and an RMSE of 0.0424 for exergy efficiency.

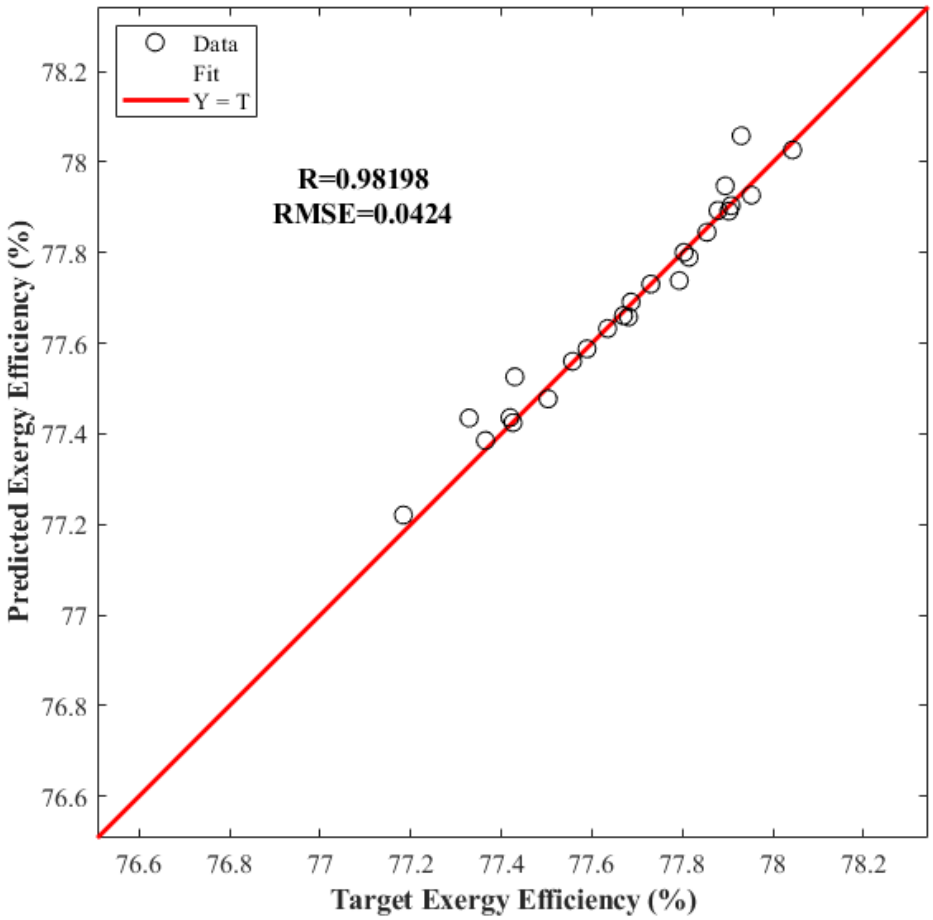

Figure 25: Predicted vs actual exergy efficiency of delayed cocking process

4.3.3 Genetic algorithm and Particle swarm based Optimization

Both the GA and PSO use ANN trained model as a surrogate to optimize the process exergy efficiency under uncertainty in process conditions. Table 11 and Table 12 present GA and PSO parameter used to optimize the process exergy efficiency.

Table 11: Genetic algorithm parameters used to optimize the exergy efficiency

GA Parameters	Integrated naphtha reforming and isomerization process	Delayed coking process
Initial population	100	20
Crossover	Over scatter	Over scatter
Crossover probability	0.8	0.8
Elite member	15	3
Mutation	Adapt feasible	Adapt feasible
Selection	Tournament	Tournament

Table 12: PSO parameters used to optimize the exergy efficiency

PSO Parameters	Integrated naphtha reforming and isomerization process	Delayed coking process
Swarm size	200	50
Min Neighbours Fraction	0.25	0.25
Self Adjustment Weight	1.49	1.49
Social Adjustment Weight	1.49	1.49
Initial Swarm Span	2000	2000

4.3.3.1 Optimization of exergy efficiency of integrated naphtha reforming and isomerization process

Table 13 shows a comparison of exergy efficiency of the process for standalone (SA), GA and PSO based frameworks. SA model refers to the first principle (FP) model of the Aspen without any optimization under uncertainty. Both the GA and PSO based frameworks outperformed the SA model in all test data samples in terms of exergy efficiency. For example, in data sample 1, the SA indicates an exergy efficiency of 50.68%, but the GA and PSO optimize it to 51.22% and 51.28%, respectively. Same case in data sample 2, where SA indicates an exergy efficiency of 50.64%, but both the GA and PSO optimize it to 51.45%, respectively.

Table 13: Comparison of SA, GA, and PSO exergy efficiency of integrated naphtha reforming and isomerization process

SR No.	SA exergy efficiency (%)	GA optimize exergy efficiency (%)	PSO optimize exergy efficiency (%)
Data Sample 1	50.68	51.22	51.28
Data Sample 2	50.64	51.45	51.45
Data Sample 3	50.55	51.22	51.28
Data Sample 4	51.02	51.46	51.47
Data Sample 5	50.37	51.26	51.27
Data Sample 6	50.75	51.44	51.45
Data Sample 7	50.71	51.28	51.46
Data Sample 8	51.10	51.46	51.47
Data Sample 9	50.82	51.46	51.46
Data Sample 10	50.79	51.28	51.44

The framework performance was cross-validated by feeding the Aspen model on the optimized process conditions derived through GA and PSO based approach and finding the absolute error. Table 14 shows a performance comparison of GA and PSO model. From Table 14, it can be validated that PSO has a slight edge over GA. For example, in data sample 1, PSO has an absolute error of -0.14% compared to GA, with an absolute error of -0.33%. As in data sample 2, PSO has an absolute error of -0.14% compared to GA, which has an absolute error of -0.90%.

Table 14: GA and PSO performance validation of integrated naphtha reforming and isomerization process

SR No.	GA exergy efficiency (%)	Aspen model validated exergy efficiency (%)	Absolute error (%)	PSO exergy efficiency (%)	Aspen model validated exergy efficiency (%)	Absolute error (%)
Data Sample 1	51.22	51.05	-0.33	51.28	51.21	-0.14
Data Sample 2	51.45	50.98	-0.90	51.45	51.38	-0.14
Data Sample 3	51.22	50.82	-0.78	51.28	50.94	-0.66
Data Sample 4	51.46	51.53	0.13	51.47	51.86	0.76
Data Sample 5	51.26	50.80	-0.90	51.27	50.94	-0.66
Data Sample 6	51.44	51.21	-0.44	51.45	51.38	-0.14
Data Sample 7	51.28	51.80	1.01	51.46	51.20	-0.50
Data Sample 8	51.46	51.54	0.15	51.47	51.77	0.60
Data Sample 9	51.46	51.26	-0.38	51.46	51.26	-0.40
Data Sample 10	51.28	51.61	0.64	51.44	51.56	0.22

4.3.3.2 Optimization of exergy efficiency of delayed coking process

Table 15 shows a comparison of exergy efficiency of the process for SA, GA and PSO based frameworks. Both the GA and PSO based frameworks outperformed the SA model in all test data samples in terms of exergy efficiency. For example, in data sample 1, the SA indicates an exergy efficiency of 77.60%, but the GA and PSO optimize it to 79.01% and 79.08%, respectively. Same case in data sample 2, where SA indicates an exergy efficiency of 77.69%, but both the GA and PSO optimize it to 77.91% and 77.94%, respectively.

Table 15: Comparison of SA, GA, and PSO exergy efficiency of delayed coking process

SR No.	SA exergy efficiency (%)	GA optimize exergy efficiency (%)	PSO optimize exergy efficiency (%)
Data Sample 1	77.28	77.96	77.97
Data Sample 2	77.60	79.01	79.08
Data Sample 3	76.97	77.91	77.94
Data Sample 4	77.88	78.30	78.36
Data Sample 5	77.90	78.76	78.78
Data Sample 6	77.55	78.61	78.62
Data Sample 7	78.01	78.30	78.37
Data Sample 8	77.78	78.66	78.76
Data Sample 9	77.90	78.83	78.87
Data Sample 10	77.83	78.71	78.77

The framework performance was cross-validated by feeding the Aspen model on the optimized process conditions derived through GA and PSO based approach and finding the absolute error. Table 16 shows a performance comparison of GA and PSO model. From Table 16, it can be validated that GA has a slight edge over PSO. For example, in data sample 1, GA has an absolute error of 0.036% compared to GA, with an absolute error of -0.04%. As in data sample 2, GA has an absolute error of -0.060% compared to PSO, which has an absolute error of 0.072%.

Table 16: GA and PSO performance validation of delayed coking process

SR No.	GA exergy efficiency (%)	Aspen model validated exergy efficiency (%)	Absolute error (%)	PSO exergy efficiency (%)	Aspen model validated exergy efficiency (%)	Absolute error (%)
Data Sample 1	77.96	77.99	0.04	77.97	78.00	-0.04
Data Sample 2	79.01	78.53	-0.60	79.08	78.51	0.73
Data Sample 3	77.91	77.93	0.02	77.94	77.98	-0.05
Data Sample 4	78.30	80.18	2.40	78.36	78.72	-0.46
Data Sample 5	78.76	78.48	-0.35	78.78	78.48	0.37
Data Sample 6	78.61	78.31	-0.38	78.62	78.45	0.21
Data Sample 7	78.30	78.65	0.44	78.37	78.66	-0.37
Data Sample 8	78.66	78.45	-0.27	78.76	78.46	0.38
Data Sample 9	78.83	78.68	-0.18	78.87	78.67	0.25
Data Sample 10	78.71	78.60	-0.13	78.77	78.60	0.22

Conclusions

The integrated process of naphtha reforming and isomerization had an overall exergy efficiency, irreversibility, and improvement potential of 50.57%, 34955.55 kW, and 17276.98 kW, respectively. The exergy destruction of naphtha reforming and isomerization units contributes 91.66% and 8.33% to overall plant exergy destruction. The reaction section had the highest irreversibility, contributing 57.30% to plantwide irreversibility. The exergy efficiency and improvement potential of the naphtha reforming unit were 44.61% and 17749.25 kW, respectively. The exergy efficiency and improvement potential of the isomerization unit were 77.38% and 659.15 kW, respectively. The delayed cocking process had an overall exergy efficiency, irreversibility, and improvement potential of 77.61%, 29204.035 kW, and 6539.51 kW, respectively. Distillation column, coker drums, and furnace contributed 50.09%, 31.31%, and 18.30% to overall plant exergy destruction and had a exergy efficiency of 64.81%, 70.31%, and 85.22%, respectively.

After exergy analysis, an ANN model was developed and used as a surrogate in a GA and PSO environment for optimization under uncertainty where exergy efficiency was the objective function. The framework outperformed SA in attaining the highest exergy efficiency. The performance of both algorithms was cross-validated by fitting the optimized conditions on the Aspen model and finding the absolute error. Overall, the performance of the GA and the PSO were comparable. The proposed integrated method enhances the feasible energy usage in reactive units and its sustainability. The current study will helps in laying a foundation for the simulation of Refinery 4.0.

Reference

[1]. S. D. O. Junior, *Exergy: production, cost and renewability*. Springer, 2012.

[2]. A. Al-Ghandoor, P. Phelan, R. Villalobos, and J. Jaber, "Energy and exergy utilizations of the US manufacturing sector," *Energy*, vol. 35, no. 7, pp. 3048-3065, 2010.

[3]. H. H. Haldorsen and P. Leach, "Energy 360: Invited perspective: The outlook for energy: A view to 2040," *Journal of Petroleum Technology*, vol. 67, no. 04, pp. 14-19, 2015.

[4]. M. A. Durrani, I. Ahmad, M. Kano, and S. Hasebe, "An artificial intelligence method for energy efficient operation of crude distillation units under uncertain feed composition," *Energies*, vol. 11, no. 11, p. 2993, 2018.

[5]. S. Brueske, C. Kramer, and A. Fisher, "Bandwidth study on energy use and potential energy saving opportunities in us petroleum refining," *Energy Efficiency and Renewable Energy (EERE): Washington, DC, USA*, 2015.

[6]. F. Bühler, T.-V. Nguyen, and B. Elmegaard, "Energy and exergy analyses of the Danish industry sector," *Applied Energy*, vol. 184, pp. 1447-1459, 2016.

[7]. E. S. Dogbe, M. A. Mandegari, and J. F. Görgens, "Exergetic diagnosis and performance analysis of a typical sugar mill based on Aspen Plus® simulation of the process," *Energy*, vol. 145, pp. 614-625, 2018.

[8]. M. Aghbashlo, H. Mobli, S. Rafiee, and A. Madadlou, "A review on exergy analysis of drying processes and systems," *Renewable and Sustainable Energy Reviews*, vol. 22, pp. 1-22, 2013.

[9]. P. Luis and B. Van der Bruggen, "Exergy analysis of energy-intensive production processes: advancing towards a sustainable chemical industry," *Journal of Chemical Technology & Biotechnology*, vol. 89, no. 9, pp. 1288-1303, 2014.

[10]. T. Taner and M. Sivrioglu, "Energy–exergy analysis and optimisation of a model sugar factory in Turkey," *Energy*, vol. 93, pp. 641-654, 2015.

[11]. N. Madlool, R. Saidur, N. Rahim, M. Islam, and M. Hossian, "An exergy analysis for cement industries: an overview," *Renewable and Sustainable Energy Reviews*, vol. 16, no. 1, pp. 921-932, 2012.

[12]. M. M. Costa, R. Schaeffer, and E. Worrell, "Exergy accounting of energy and materials flows in steel production systems," *Energy*, vol. 26, no. 4, pp. 363-384, 2001.

[13]. V. Costa, L. Tarelho, and A. Sobrinho, "Mass, energy and exergy analysis of a biomass boiler: A portuguese representative case of the pulp and paper industry," *Applied Thermal Engineering*, vol. 152, pp. 350-361, 2019.

[14]. G. BoroumandJazi, B. Rismanchi, and R. Saidur, "A review on exergy analysis of industrial sector," *Renewable and Sustainable Energy Reviews*, vol. 27, pp. 198-203, 2013.

[15]. M. R. Rahimpour, M. Jafari, and D. Iranshahi, "Progress in catalytic naphtha reforming process: A review," *Applied energy*, vol. 109, pp. 79-93, 2013.

[16]. M. Mohamed, W. Shehata, A. A. Halim, and F. Gad, "Improving gasoline quality produced from MIDOR light naphtha isomerization unit," *Egyptian Journal of Petroleum*, vol. 26, no. 1, pp. 111-124, 2017.

[17]. D. S. Jones, "Elements of petroleum processing," 1995.

[18]. C. Liang and X. Feng, "Heat integration of a continuous reforming process," *Chemical Engineering Transactions*, vol. 25, pp. 213-218, 2011.

[19]. L. M. Ulyev, P. O. Kapustenko, and D. D. Nechiporenko, "The Choice of the Optimal Retrofit Method for Sections of the Catalytic Reforming Unit," 2014.

[20]. B. S. Babaqi, M. S. Takriff, N. T. A. Othman, and S. K. Kamarudin, "Yield and energy optimization of the continuous catalytic regeneration reforming process based particle swarm optimization," *Energy*, vol. 206, p. 118098, 2020.

[21]. R. G. Falcón, D. V. Alonso, L. G. Fernández, and L. Pérez-Lombard, "Improving energy efficiency in a naphtha reforming plant using Six Sigma methodology," *Fuel processing technology*, vol. 103, pp. 110-116, 2012.

[22]. D. Velázquez, R. González-Falcón, L. Pérez-Lombard, L. M. Gallego, I. Monedero, and F. Biscarri, "Development of an energy management system for a naphtha reforming plant: A data mining approach," *Energy conversion and management*, vol. 67, pp. 217-225, 2013.

[23]. X. Feng, J. Pu, J. Yang, and K. H. Chu, "Energy recovery in petrochemical complexes through heat integration retrofit analysis," *Applied Energy*, vol. 88, no. 5, pp. 1965-1982, 2011.

[24]. Z. Ghazizahedi and M. Hayati-Ashtiani, "Heat transfer enhancement to decrease the energy consumption of a Light Naphtha Isomerization unit by

means of heat exchanger network retrofitting," in *IOP Conference Series: Materials Science and Engineering*, 2018, vol. 433, no. 1: IOP Publishing, p. 012070.

[25]. A. T. Jarullah, F. M. Abed, A. M. Ahmed, and I. M. Mujtaba, "Optimisation of several industrial and recently developed AJAM naphtha isomerization processes using model based techniques," *Computers & Chemical Engineering*, vol. 126, pp. 403-420, 2019.

[26]. Z. Ghazizahedi and M. Hayati-Ashtiani, "Retrofitting isomerization process to increase gasoline quality and decrease CO2 emission along with energy analysis using Pinch Technology," *Energy Sources, Part A: Recovery, Utilization, and Environmental Effects*, pp. 1-12, 2020.

[27]. Y. Li, X. Wang, and X. Feng, "Heat Integration of a Delayed Coking Plant," in *2009 International Conference on Energy and Environment Technology*, 2009, vol. 1: IEEE, pp. 687-690.

[28]. Y. Lei, X. Qi, B. Zhang, Q. Chen, and C. W. Hui, "Simultaneous optimization of the complex fractionator and heat exchanger network considering the constraints of variable heat removals in delayed coking units," *Industrial & Engineering Chemistry Research*, vol. 53, no. 33, pp. 13073-13086, 2014.

[29]. D. Sidenev, S. Savelyev, A. Valyeva, A. Gaysina, and R. Khasanov, "Enhancing the Heat Exchange Efficiency of a Delayed Coking Unit," *Chemistry and Technology of Fuels and Oils*, vol. 58, no. 3, pp. 444-448, 2022.

[30]. R. Rivero, "Application of the exergy concept in the petroleum refining and petrochemical industry," *Energy conversion and Management*, vol. 43, no. 9-12, pp. 1199-1220, 2002.

[31]. J.-F. Portha, S. Louret, M.-N. Pons, and J.-N. Jaubert, "Estimation of the environmental impact of a petrochemical process using coupled LCA and exergy analysis," *Resources, Conservation and Recycling*, vol. 54, no. 5, pp. 291-298, 2010.

[32]. J. Mustafa, I. Ahmad, M. Ahsan, and M. Kano, "Computational fluid dynamics based model development and exergy analysis of naphtha reforming reactors," *International Journal of Exergy*, vol. 24, no. 2-4, pp. 344-363, 2017.

[33]. Q. Chen, Q. Yin, S. Wang, and B. Hua, "Energy-use analysis and improvement for delayed coking units," *Energy*, vol. 29, no. 12-15, pp. 2225-2237, 2004.

[34]. Y. Lei, D. Zeng, and G. Wang, "Improvement potential analysis for integrated fractionating and heat exchange processes in delayed coking units," *Chinese journal of chemical engineering*, vol. 24, no. 8, pp. 1047-1055, 2016.

[35]. M. S. Arif and I. Ahmad, "Artificial intelligence based prediction of exergetic efficiency of a blast furnace," in *Computer Aided Chemical Engineering*, vol. 50: Elsevier, 2021, pp. 1047-1052.

[36]. M. Khan, I. Ahmad, M. Ahsan, M. Kano, and H. Caliskan, "Prediction of optimum operating conditions of a furnace under uncertainty: An integrated framework of artificial neural network and genetic algorithm," *Fuel*, vol. 330, p. 125563, 2022.

[37]. S. Kurban, G. K. Kaya, and S. Yaman, "Exergy Analysis of Vacuum Distillation Unit," in *Computer Aided Chemical Engineering*, vol. 50: Elsevier, 2021, pp. 63-68.

[38]. A. U. Akram, I. Ahmad, A. Chughtai, and M. Kano, "Exergy analysis and optimisation of naphtha reforming process with uncertainty," *Int. J. Exergy*, vol. 26, pp. 247-262, 2018.

[39]. J. Szargut, D. R. Morris, and F. R. Steward, "Exergy analysis of thermal, chemical, and metallurgical processes," 1987.

[40]. E. Sciubba and G. Wall, "A brief commented history of exergy from the beginnings to 2004," *International Journal of Thermodynamics*, vol. 10, no. 1, pp. 1-26, 2007.

[41]. A. Naeimi, M. Bidi, M. H. Ahmadi, R. Kumar, M. Sadeghzadeh, and M. A. Nazari, "Design and exergy analysis of waste heat recovery system and gas engine for power generation in Tehran cement factory," *Thermal Science and Engineering Progress*, vol. 9, pp. 299-307, 2019.

[42]. F. Shen, M. Wang, L. Huang, and F. Qian, "Exergy analysis and multi-objective optimisation for energy system: a case study of a separation process in ethylene manufacturing," *Journal of Industrial and Engineering Chemistry*, vol. 93, pp. 394-406, 2021.

[43]. A. Al-Shathr, Z. M. Shakor, H. S. Majdi, A. A. AbdulRazak, and T. M. Albayati, "Comparison between Artificial Neural Network and Rigorous Mathematical Model in Simulation of Industrial Heavy Naphtha Reforming Process," *Catalysts*, vol. 11, no. 9, p. 1034, 2021.

[44]. T. Gueddar and V. Dua, "Novel model reduction techniques for refinery-wide energy optimisation," *Applied energy*, vol. 89, no. 1, pp. 117-126, 2012.

[45]. Z. U. Haq, H. Ullah, M. N. A. Khan, S. R. Naqvi, and M. Ahsan, "Hydrogen Production Optimization from Sewage Sludge Supercritical Gasification Process using Machine Learning Methods Integrated with Genetic Algorithm," *Chemical Engineering Research and Design*, 2022.

[46]. H. P. Gavin, "The Levenberg-Marquardt algorithm for nonlinear least squares curve-fitting problems," *Department of Civil and Environmental Engineering, Duke University*, vol. 19, 2019.

[47]. S. Katoch, S. S. Chauhan, and V. Kumar, "A review on genetic algorithm: past, present, and future," *Multimedia Tools and Applications*, vol. 80, no. 5, pp. 8091-8126, 2021.

[48]. R. Woodward and E. J. Kelleher, "Towards 'smart lasers': self-optimisation of an ultrafast pulse source using a genetic algorithm," *Scientific reports*, vol. 6, no. 1, pp. 1-9, 2016.

[49]. M. Kumar, D. Husain, N. Upreti, and D. Gupta, "Genetic algorithm: Review and application," *Available at SSRN 3529843*, 2010.

[50]. K. Jebari and M. Madiafi, "Selection methods for genetic algorithms," *International Journal of Emerging Sciences*, vol. 3, no. 4, pp. 333-344, 2013.

[51]. G. K. Soon, T. T. Guan, C. K. On, R. Alfred, and P. Anthony, "A comparison on the performance of crossover techniques in video game," in *2013 IEEE international conference on control system, computing and engineering*, 2013: IEEE, pp. 493-498.

[52]. M. Yousefi, M. Omid, S. Rafiee, and S. Ghaderi, "Strategic planning for minimizing CO2 emissions using LP model based on forecasted energy demand by PSO Algorithm and ANN," *International Journal of Energy and Environment (Print)*, vol. 4, 2013.

[53]. P. Duchêne, L. Mencarelli, and A. Pagot, "Optimization approaches to the integrated system of catalytic reforming and isomerization processes in petroleum refinery," *Computers & Chemical Engineering*, vol. 141, p. 107009, 2020.

[54]. T. J. Kotas, *The exergy method of thermal plant analysis*. Paragon Publishing, 2012.

[55]. M. Nakaiwa, K. Huang, A. Endo, T. Ohmori, T. Akiya, and T. Takamatsu, "Internally heat-integrated distillation columns: a review," *Chemical Engineering Research and Design*, vol. 81, no. 1, pp. 162-177, 2003.

[56]. C. Yan, L. Lv, A. Eslamimanesh, and W. Shen, "Application of retrofitted design and optimization framework based on the exergy analysis to a crude oil distillation plant," *Applied Thermal Engineering*, vol. 154, pp. 637-649, 2019.

[57]. I. López Paniagua, J. Rodríguez Martín, C. González Fernandez, Á. Jiménez Alvaro, and R. Nieto Carlier, "A new simple method for estimating exergy destruction in heat exchangers," *Entropy*, vol. 15, no. 2, pp. 474-489, 2013.

[58]. S. A. Ashrafizadeh, M. Amidpour, and M. Abolmashadi, "Exergy analysis of distillation column using concept of driving forces," *Journal of chemical engineering of Japan*, vol. 46, no. 7, pp. 434-443, 2013.

[59]. A. Szklo and R. Schaeffer, "Fuel specification, energy consumption and CO2 emission in oil refineries," *Energy*, vol. 32, no. 7, pp. 1075-1092, 2007.

[60]. A. Ghannadzadeh and M. Sadeqzadeh, "Exergy analysis as a scoping tool for cleaner production of chemicals: a case study of an ethylene production process," *Journal of Cleaner Production*, vol. 129, pp. 508-520, 2016.

[61]. D. Iranshahi, M. Jafari, R. Rafiei, M. Karimi, S. Amiri, and M. R. Rahimpour, "Optimal design of a radial-flow membrane reactor as a novel configuration for continuous catalytic regenerative naphtha reforming process considering a detailed kinetic model," *International journal of hydrogen energy*, vol. 38, no. 20, pp. 8384-8399, 2013.

[62]. A. Doldersum, "Exergy analysis proves viability of process modifications," *Energy Conversion and Management*, vol. 39, no. 16-18, pp. 1781-1789, 1998.